Types of Turbomachinery Best Suited for Space Missions Requiring Power Outputs in the Range of Few Kw to 1 Mw

By

AMMAR BENGUEDOUAR
Ing., Ecole Nationale Polytechnique d'Alger
(1984)

Submitted in Partial Fulfillment
of the Requirements for the
Degree of

Master of Science in
Aeronautics and Astronautics

at the

Massachusetts Institute of Technology
February 1988

Signature of Authc _____
Department of Aeronautics and Astronautics
December , 1987

Certified by _____ 0 JAN 88
Prof. Jean F. Louis
Thesis Supervisor , Department of Aeronautics and Astronautics

Accepted by _____
Prof. Harold Y. Wachman
Chairman , Department Graduate Committee

Types of Turbomachinery Best Suited for Space Missions Requiring Power Outputs in the Range of Few Kw to 1 Mw

By

Ammar Benguedouar

Submitted to the Department of Aeronautics and Astronautics
in December, 1987 in Partial Fulfillment of the
Requirements for the Degree of Master of Science in
Aeronautics and Astronautics

ABSTRACT

The weight and the efficiency of a space power generation system are very important parameters, but it was found that the turbine and the compressor weight was very small compared to that of the whole system. Therefore the efficiency alone can be a figure of merit while choosing the type of the turbine or the compressor.

This subject deals with the choice of the most efficient turbines for given parameters and conditions of use. The NsDs-diagrams were used to plot the maximum efficiency for different specific speeds for both radial and axial turbines. It was found that the radial turbines have maximum efficiency for specific speeds between 50 and 90, and the axial turbines have maximum efficiency for specific speeds greater than 90.

The specific speed is also proportional to the net output power. Taking into account the higher limit of the radial turbines specific speed, the power limit at which the radial turbines have better efficiency than the axial turbines is 300 kw.

Concerning the compressors, NsDs-diagrams show that for specific speeds between 90 and 130 the radial compressors are the most efficient compressors. For specific speeds between 130 and 300 the mixed flow compressors are the most efficient compressors. For specific speeds greater than 300 the axial flow compressors the most efficient compressors

Using the NsDs-diagrams another factor called specific diameter can be obtained and from which the size and the approximate weight of the turbine are calculated.

Thesis supervisor : Jean F. Louis
Title : Professor of Aeronautics and Astronautics.

ACKNOWLEDGEMENTS

I would like to thank my thesis supervisor, Professor Jean F. Louis, for his guidance and his advice that he was giving me during this thesis work and during the courses I took with him.

I would like also to thank the Algerian government for the financial supprt and for making my life easy during my stay in the United States.

Finally, I thank my parents and my whole family and all my friends.

TABLE OF CONTENTS

NOMENCLATURE

A:	Cross sectional area
a:	Sonic velocity
C:	Absolute velocity
Cm:	Torque coefficient
D:	Diameter
Ds:	Specific diameter
F:	Frictional force
F_t:	Specific weight, Kg/Kw
H:	Total enthalpy
h:	Static enthalpy
h_e:	Head, m
h_{fric}:	Energy lost by friction
HP:	Power in horse power
I:	Rothalpy
L:	Length of the mean flow line
M:	Mach number
$\dot{m}$:	Mass flow
n_v:	Number of vanes in the impeller
N:	Rotational speed
Ns:	Specific speed
P:	Total pressure

p:	Static pressure
P_{disc}:	Power necessary to rotate the disc.
P_s:	Shaft power
Q	Volume flow rate
r:	Radius
R:	Reaction
Re:	Reynolds number
SF:	Slip factor
τ:	Torque
τ_{tan}:	Tangential component of the shear stress between the disc and the fluid
T:	Temperature
U:	Blade speed
v:	Specific volume
Wc:	Specific work
We:	Engine total weight
w:	Relative velocity
X:	Total resistive torque of the two sides of the disc
y:	Perimeter of the flow section
Y_t:	Turbine pressure ratio coefficient
Y_C:	Compressor pressure ratio coefficient
Z:	Number of blades
α:	Flow angle
β':	Gas angle

β:	Geometric vane exit angle
γ:	Ratio of specific heats
η:	Efficiency
Ω, ω:	Angular velocity.
ρ:	Density
ξ:	Work input coefficient
ϕ;	Flow coefficient
ξ_N:	Nozzle enthalpy loss coefficient
ξ_R:	Rotor enthalpy loss coefficient
Ψ_N:	Nozzle velocity coefficient
Ψ_R:	Rotor velocity coefficient.
λ:	Drag coefficient.

LIST OF FIGURES

CHAPTER 1.INTRODUCTION

1.1. CENTRIFUGAL COMPRESSORS

1.1.1. INTRODUCTION

The earliest machines used the centrifugal compressor. Development of centrifugal compressors continued into the mid 1950's, but after development of technology, axial flow compressors took place because of their higher efficiency and higher pressure ratios needed for aircrafts.

At very low air mass flow rates the efficiency of axial compressors drops sharply, tip clearance is very big relative to the size of the blade. Therefore the losses to this phenomenon are high. The blades are very small and difficult to be made accurately and the advantage lies with the centrifugal compressors.

In the mid 1960's the need for advanced military helicopters powered by small gas turbine engines provided the necessary impetus for further rapid development of the centrifugal compressor.

Recent performance data for small single stage centrifugal compressors quotes total to static efficiencies of 80 - 84 % for pressure ratios between 4 and 6 to 1. Higher pressure ratios than this have been achieved in single stages but at reduced efficiency and small airflow range.

1.1.2. Principal of Functioning of Centrifugal Compressor

A centrifugal compressor consists essentially of a rotating impeller followed by diffuser. Fig. 1.1 below shows the various elements of a centrifugal compressor.

Fluid is drawn in through the inlet casing into the eye of the impeller. The function of the impeller is to increase the energy level of the fluid by whirling it outward, thereby increasing the angular momentum of the fluid.

The feature which distinguishes the centrifugal compressor from the axial compressor is that the angular momentum of the fluid flowing through the impeller is increased partly by virtue of the impeller outlet diameter being significantly larger than its inlet diameter. All work done to the gas must be done by the active element , the impeller. The stationary element is passive, that is, it cannot contribute any additional energy to the stage. It can only convert the energy and unfortunately contribute to the losses. Both the static pressure and velocity are increased within the impeller.

The purpose of the diffuser is to convert the kinetic energy of the fluid leaving the impeller into pressure energy.

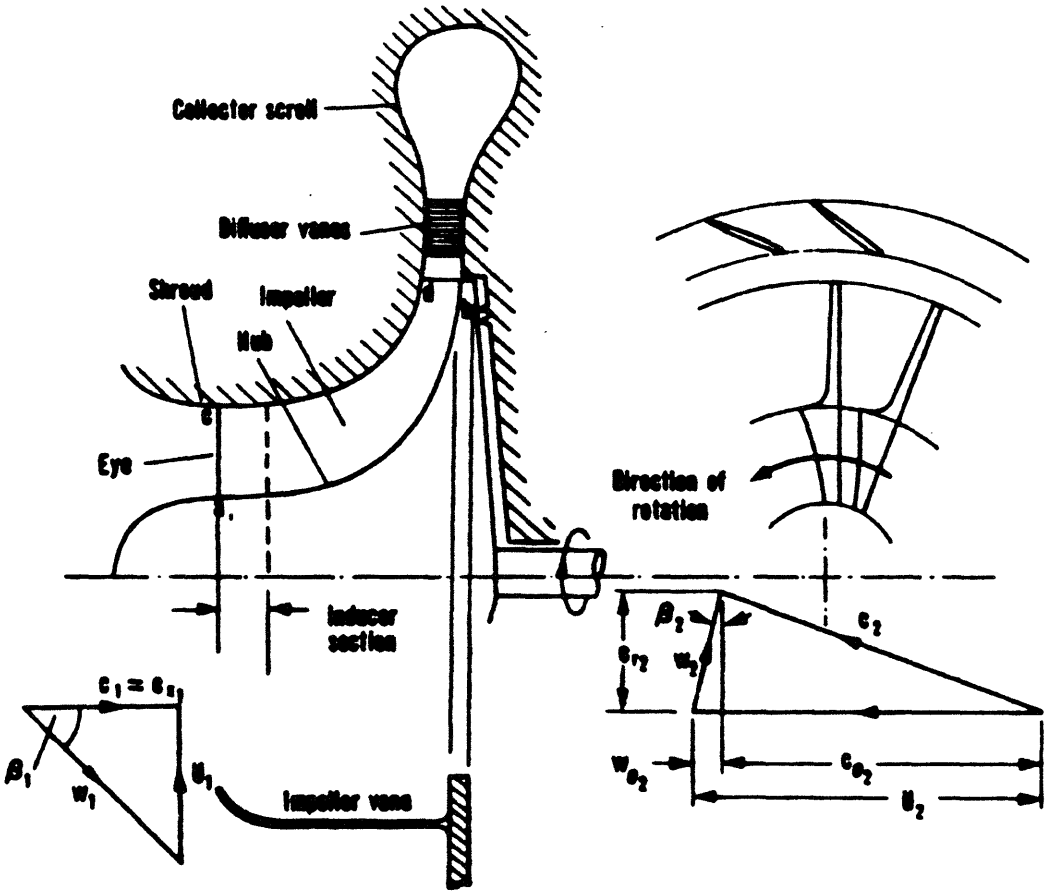

Fig. 1.1.Centrifugal compressor stage and velocity diagrams at impeller entry and exit.

Outside the diffuser is a scroll or volute whose function is to collect the flow from the diffuser and deliver it to the outlet pipe.

On fig. 1.1. the curved surface of revolution (a - b) of the impeller is called the *hub*. The curved surface (c - d) forming the outer boundary to the flow of fluid is called the *shroud.*

Impellers may be enclosed by having the shroud attached to the vane ends (called shrouded impellers), or unenclosed with a small clearance gap between the vane ends and the stationary wall. Shrouding an impeller has the merit of eliminating tip leakage losses, but it has been demonstrated to be detrimental at high speeds and beneficial at low speeds of rotation.

1.1.3.Theoretical Analysis of Centrifugal Compressors

1.1.3.1. Inlet Casing :

In this part the fluid is accelerated from velocity C_0 to velocity C_1. Some energy in the inlet casing is being transformed to kinetic energy and the pressure drops from P_0 to P_1. See figure (1.2.) below.
Stagnation enthalpy throughout the inlet casing is constant , then

$$h_{oo} = h_{o1}$$

$$h_o + 1/2\, C_o^2 = h_1 + 1/2\, C_1^2 \qquad (1.1)$$

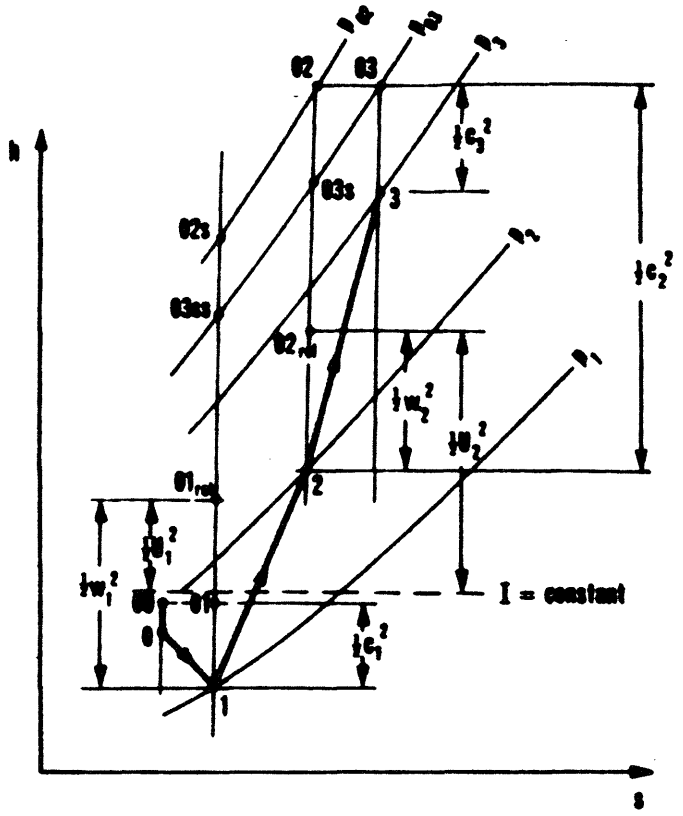

Fig. 1.2. Mollier Diagram for the Complete Centrifugal Compressor Stage.

1.1.3.2. Impeller

Swirling fluid enters the control volume of the impeller at radius r_1 with tangential velocity $C_{\theta 1}$ and leaves it at radius r_2 with tangential velocity $C_{\theta 2}$. The sum of the moments of the external forces acting on the fluid is :

$$\tau_a = \dot{m} (r_2 C_{\theta 2} - r_1 C_{\theta 1}) \qquad (1.2)$$

If the impeller turns at Ω angular velocity, the rate at which it does work on the fluid for a one-dimensional case is :

$$\tau_a \Omega = \dot{m} (U_2 C_{\theta 2} - U_1 C_{\theta 1}) = W_c \qquad (1.3)$$

where :

$$U_2 = \Omega r_2$$
$$U_1 = \Omega r_1.$$

The work done on the fluid is :

$$\Delta w_c = \frac{W_c}{\dot{m}} = U_2 C_{\theta 2} - U_1 C_1 = h_{02} - h_{01} \qquad (1.4)$$

I : is the rothalpy, it is constant throughout the impeller,

U : is the blade speed,

W_c : is the specific work.

In three-dimensional motion :

$$C^2 = C_r^2 + C_\theta^2 + C_x^2 \qquad (1.5)$$

substituting C^2 in rothalpy we get :

$$I = h + 1/2 (C_r^2 + C_\theta^2 + C_x^2 - 2 U C_\theta) \qquad (1.6)$$

adding and substituting $1/2\ U^2$ we get:

$$I = h + 1/2 [(U - C_\theta)^2 + C_r^2 + C_x^2 - U^2] \qquad (1.7)$$

but

$U - C_\theta = w_\theta$ (from velocity triangles shown on fig. 1.1)

Since :

$$w^2 = C_r^2 + w_\theta^2 + C_x^2 \qquad (1.8)$$

the rothalpy becomes:

$$I = h + 1/2 (w^2 - U^2) \qquad (1.9)$$

Since the rothalpy is constant throughout the impeller then :

$$I_1 = I_2$$

and

$$h_2 - h_1 = 1/2 (U_2^2 - U_1^2)\ 1/2 (w_1^2 - w_2^2) \qquad (1.10)$$

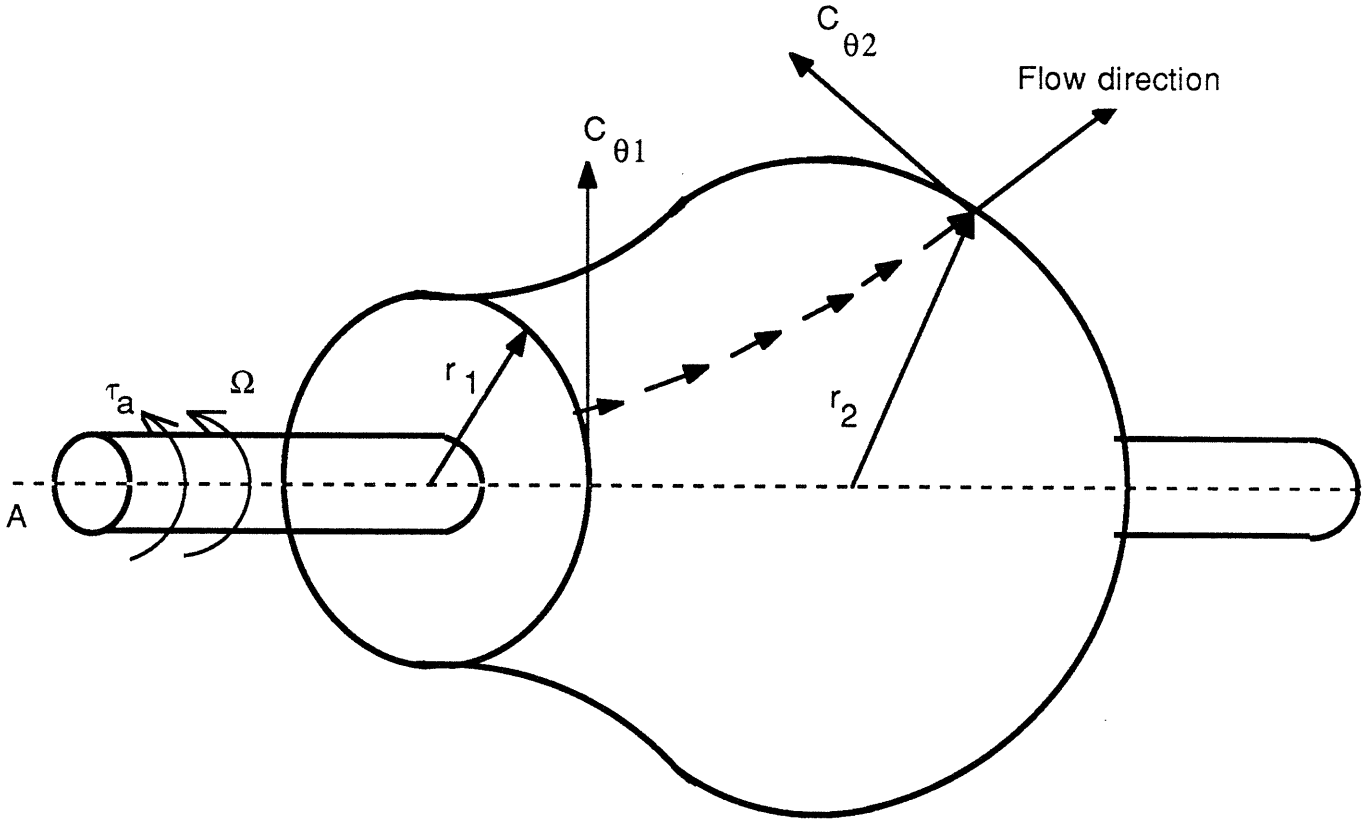

Fig.1.3. Control volume for a generalized turbomachine

1.1.3.3. The Diffuser.

In this portion the pressure is raised from p_2 to p_3 by decelerating adiabatically the fluid coming from the velocity C_2 to velocity C_3, in the mean time the stagnation enthalpy is remained constant through the diffuser,

$$h_{02} = h_{03}$$

$$h_2 + 1/2\, C_2^{\,2} = h_3 + 1/2\, C_3^{\,2}$$

$$C_2 > C_3$$

1.1.4.Energy Losses in the Stage

The energy losses are divided into aerodynamic losses, disc friction losses, leakage losses, and mechanical losses.

1.1.4.1. Aerodynamic losses:

Due to fluid friction to the surfaces of the flow passages some energy is being lost .

If :

C = absolute velocity.

The energy lost is given by :

$$h_{fric} = \frac{f\, C^2\, y\, L}{8A} \qquad (1.11)$$

where :

f: is the frictional factor given by Prandtl , Van Karman and Nikuradse as:

$$\text{Log}_{10}\,\text{Re} = \frac{1}{2}\left(\sqrt{\frac{1}{f}} - \text{Log}_{10}\,f\right) + 0.4 \qquad (1.12)$$

A = cross sectional area

L = length of the mean flow line

y : is the perimeter of the flow section

1.1.4.2. Disc Friction Losses:

The total resistive torque is given by [16]:

$$X = 2\int_{r_1}^{r_2} \tau_{tan}\, 2\pi\, r^2\, dr \qquad (1.15)$$

where :

τ_{tan} = the tangential component of the shear stress between the disc and the fluid.

X = the total resistive torque of the two sides of the disc.

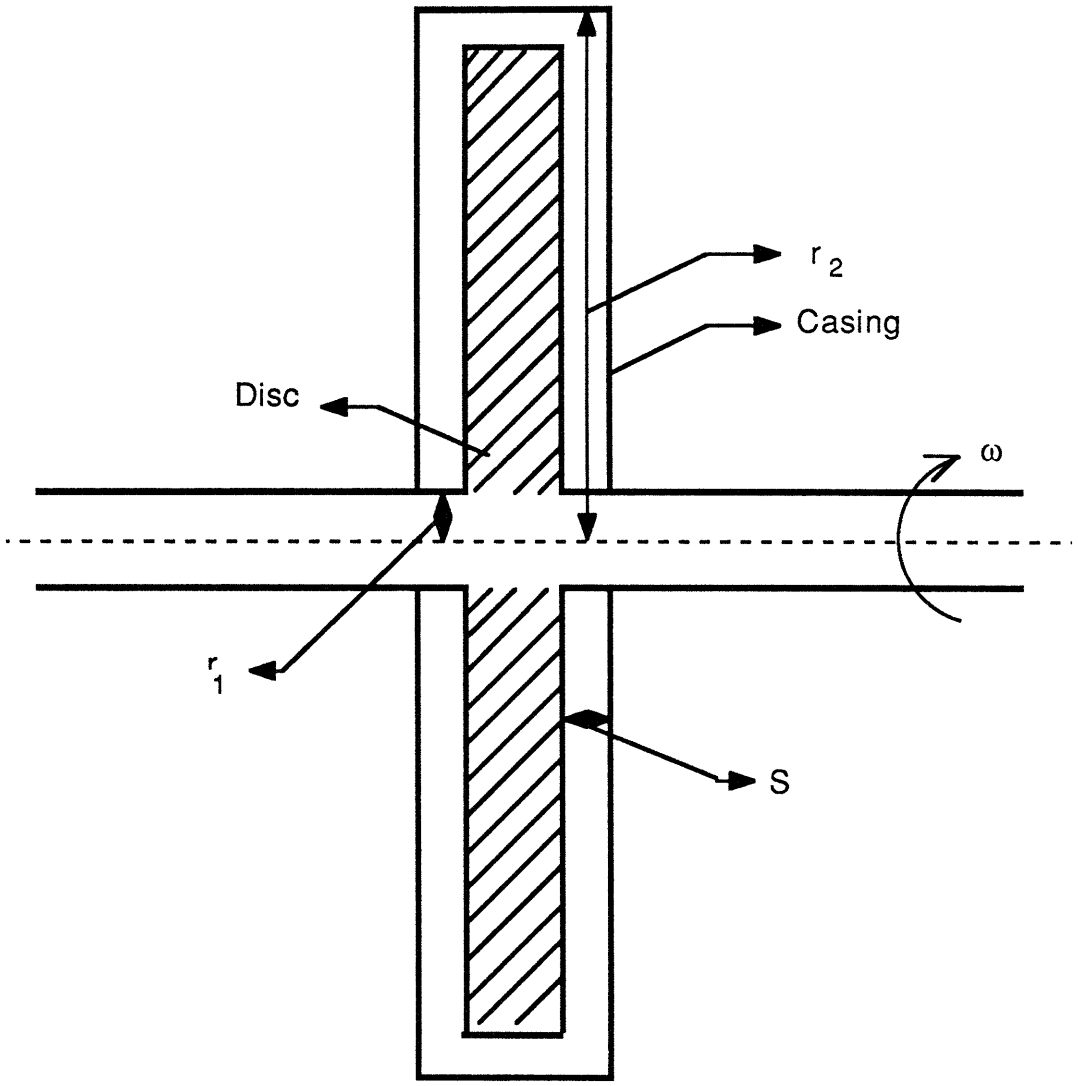

Fig.1.5. Enclosed rotating disc.

Due to the torque X an input power P_{disc} is necessary to rotate the disc at angular velocity ω. The input power necessary to rotate the disc is :

$$P_{disc} = 2\int_{r_1}^{r2} 2\pi\, \tau_{tan}\, r^2\, \omega\, dr \qquad (1.16)$$

Experiments give an estimation to P_{disc} by calculating the total resistive torque from a non-dimensional torque coefficient *Cm* plotted as a function of Reynolds number and disc casing ratio (S / r_2). the total resistive torque X is given by [16]:

$$X = 1/2\, Cm\, \rho\, \omega^2 (r_2^5 - r_1^5) \qquad (1.17)$$

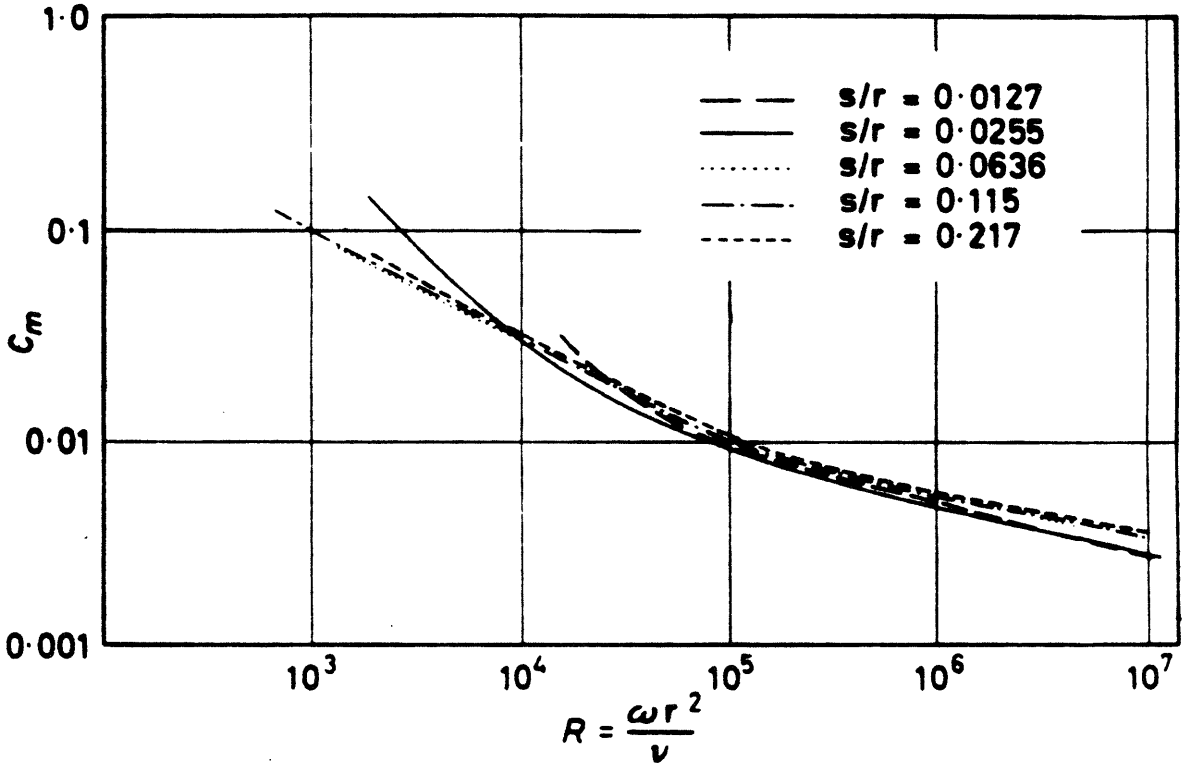

Fig.1.6. Smooth disc torc coefficient.

1.1.4.3. Leackage Losses:

The leakage occurs at the sections where the shaft passes through the casing and at the outer radius of the eye from the impeller casing back into the eye.

There are methods to minimize the leakage losses. One of these methods is to make the gap as small as possible, but this will increase the friction losses.

An other method to minimize the leakage losses, and not at the expense of energy losses by friction, is to fit labyrinth glands, either staggered or straight through, in the gap.

Considering the flow through two adjacent constructions as shown on figure (1.8), we have :

$$h_0 + C_0^2 / 2 = h1 + C_1^2 / 2$$

Before the constriction 1 as shown on the figure the velocity is considered zero

$$C_0 = 0$$

Then

$$h_0 = h_1 + C_1^2 / 2$$

$$h_0 - h_1 = C_1^2 / 2$$

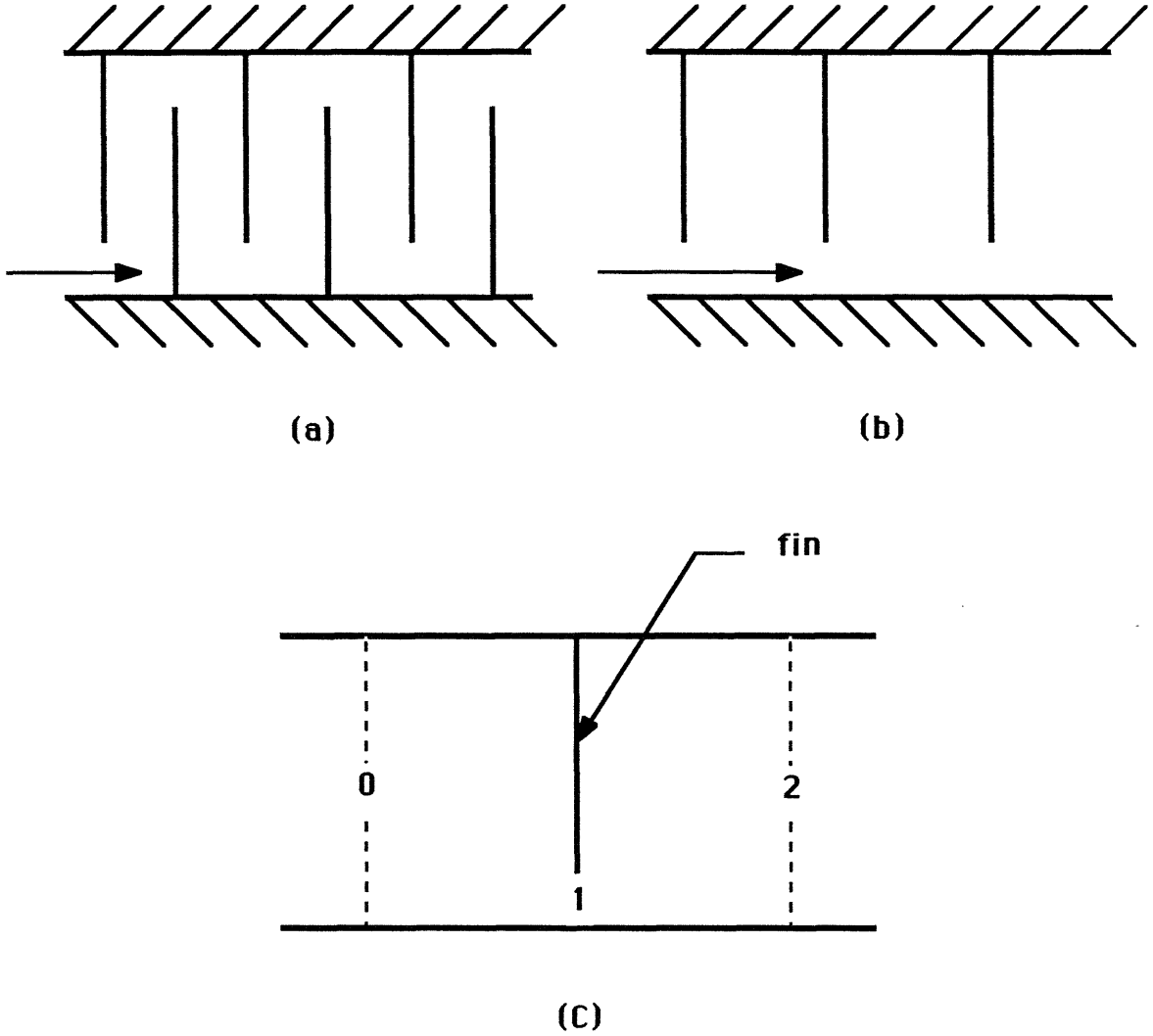

Fig. 1-7. Labyrinth glands: (a) staggered; (b) straight through; (c) flow model -- (0 to 1), isentropic; (1 to 2) kinetic energy transformed to internal energy at constant pressure.

We have

$$\Delta h_{01} = \frac{\gamma}{\gamma - 1} p_0 V_0 \left[\left(\frac{p_4}{p_0} \right)^{\frac{\gamma - 1}{\gamma}} - 1 \right]$$

From the continuity equation :

$$\dot{m} = \frac{A_1 C_1}{v_1}$$

Then :

$$\Delta h_{01} = -\frac{C_1^2}{2} = -\frac{1}{2} \left(\frac{\dot{m} v_1}{A_1} \right)^2$$

Hence

$$\left(\frac{\dot{m}}{A_1} \right)^2 = -2 \frac{\gamma}{\gamma - 1} \frac{p_0 v_0}{v_1^2} \left[\left(\frac{p_1}{p_0} \right)^{\frac{\gamma - 1}{\gamma}} - 1 \right]$$

Where :

v : is the specific volume (m^3 / kg)

Since we have 0 - 1 an isentropic transformation then :

$$p_o v_o^{\gamma} = p_1 v_1^{\gamma}$$

$$vo / v1 = (p1 / po)^{1/\gamma}$$

Then :

$$\left(\frac{\dot{m}}{A_1} \right)^2 = -2 \frac{\gamma}{\gamma - 1} \frac{p_0}{v_0} \left[\left(\frac{p_1}{p_0} \right)^{\frac{\gamma-1}{\gamma}} - 1 \right]$$

With some transformations in this expression we get :

$$\left(\frac{\dot{m}}{A_1} \right)^2 = 2 \frac{\gamma}{\gamma - 1} \frac{p_o}{v_o} \left[\left(\frac{p_1}{p_o} \right)^{\frac{2}{\gamma}} - \left(\frac{p_1}{p_o} \right)^{\frac{\gamma+1}{\gamma}} \right] \qquad (1.22)$$

Now if $A_3 = A_1$ then

$$\left(\frac{\dot{m}}{A_3} \right)^2 = 2 \frac{\gamma}{\gamma - 1} \frac{p_2}{v_2} \left[\left(\frac{p_3}{p_2} \right)^{\frac{2}{\gamma}} - \left(\frac{p_3}{p_2} \right)^{\frac{\gamma+1}{\gamma}} \right] \qquad (1.22)$$

Since

$$A1 = A3$$

See figure (1.8).

Then equating equations (1.21) and (1.22) we get :

$$\frac{p_o}{V_o}\left[\left(\frac{p_1}{p_o}\right)^{\frac{2}{\gamma}}-\left(\frac{p_1}{p_o}\right)^{\frac{\gamma+1}{\gamma}}\right]=\frac{p_2}{V_2}\left[\left(\frac{p_3}{p_2}\right)^{\frac{2}{\gamma}}-\left(\frac{p_3}{p_2}\right)^{\frac{\gamma+1}{\gamma}}\right] \qquad (1.23)$$

Since

$$p_1 = p_2 \quad \text{and} \quad p_3 = p_4$$

Substituting into equation (1 23) and taking into account that all kinetic energy is converted into internal energy then :

$$T_o = T_2$$

From :

$$p\,v = r\,T$$

we have

$$p_o\,v_o = r\,T_o$$

$$p_2\,v_2 = r\,T_2$$

Then

$$v_2 / v_o = p_o / p_2 \qquad (1.24)$$

Finally substituting (1.24) in (1.23) we get.

$$\left[\left(\frac{p_2}{p_0}\right)^{\frac{2}{\gamma}}-\left(\frac{p_2}{p_0}\right)^{\frac{\gamma+1}{\gamma}}\right]\left(\frac{p_0}{p_2}\right)^2=\left[\left(\frac{p_4}{p_2}\right)^{\frac{2}{\gamma}}-\left(\frac{p_4}{p_2}\right)^{\frac{\gamma+1}{\gamma}}\right] \qquad (1.25)$$

This formula gives a connection between the pressure ratios of the two adjacent constructions.

To find the pressure ratio between the first and last construction (the whole seal), we keep calculating the pressure ratios between every two adjacent constructions, and the product of all pressure ratios found is the pressure ratio of the entire seal.

1.1.5. Slip Factor:

The flow in an impeller is not completely guided by the vanes and hence the effective fluid outlet angle does not equal the vane outlet angle. And this is due to an acceleration force called the *coriolis* component of the acceleration. This is defined as the acceleration due to the relative motion of the particle superimposed

on the wheel's rotation. This acceleration is normal to the passage and has a magnitude of ($2 w \omega$) [25 , 28].

To account for this deviation a factor known as *slip factor* is used to correct the energy transfer calculated. The leaving angle β_2' is the gas angle.

The slip factor is obtained by Stodola equation which is an equation used in practical design prior to the advent of the more sophisticated methods available now.

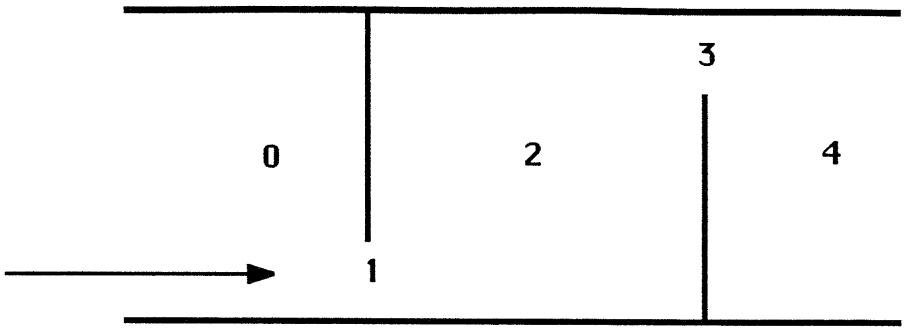

Fig. 1.8. Flow through two adjacent constructions.

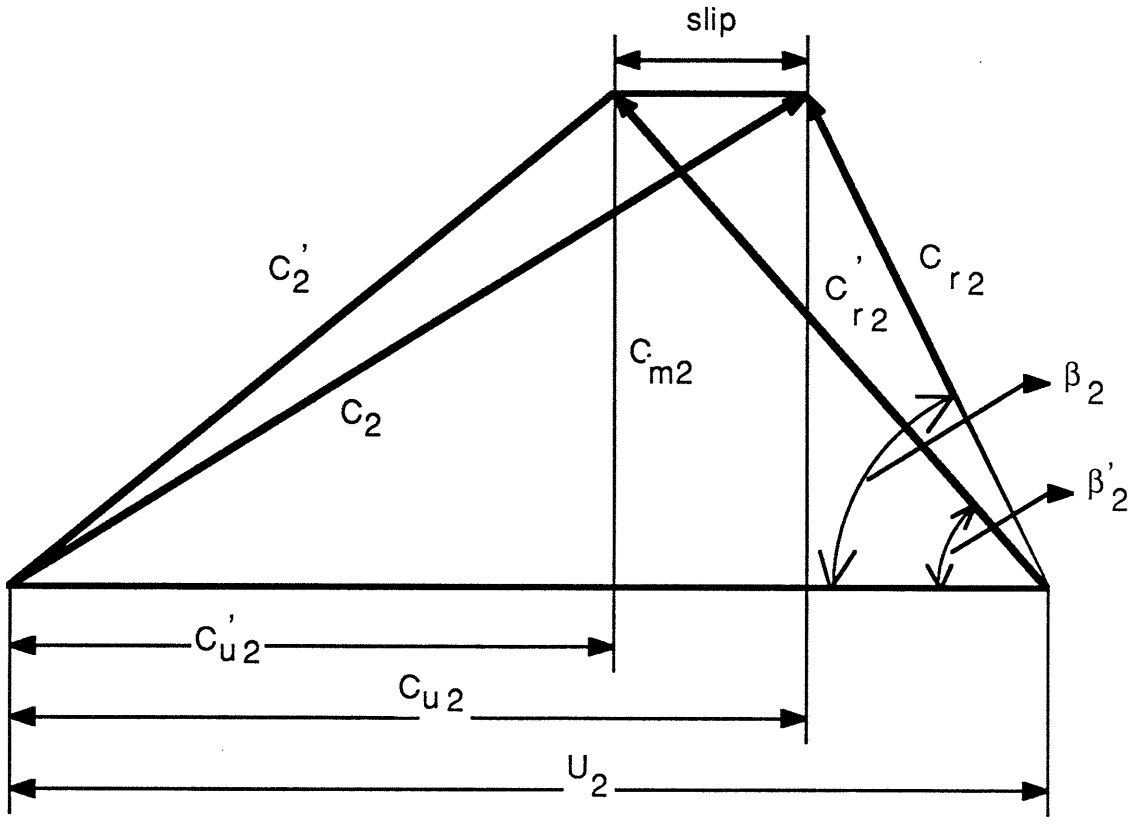

Fig. 1.9. Discharge velocity vector triangle showing the effect of *slip*.

Returning to the velocity triangles, seen on the figure:

C_2' : is the gas absolute velocity with slip,

C_2 : is the gas absolute velocity without slip,

β_2' : is the gas angle with slip ,

β_2 : is the geometric vane exit angle,

C_{u2} and C_{u2}' : tangential components of the absolute velocity

U_2 : is the impeller tip velocity.

The Stodola slip factor [15] is defined as :

$$\text{Slip} = U_2 (\pi \text{ Sin } \beta_2) / n_v$$

where:

n_v : number of vanes in the impeller.

The slip factor is then:

$$SF = C_{u2}' / C_{u2} \qquad (1.27)$$

Since:

$$C_{u2}' = C_{u2} - \text{slip}$$

Then

$$SF = (C_{u2} - \text{slip})$$

$$SF = 1 - \frac{U_2}{C_{u2}}\left(\frac{\pi \sin \beta_2}{n_v}\right) \qquad (1.28)$$

1.1.5.1. Effect of slip factor on work input

The ideal work input coefficient is given by :

$$\zeta_i = C_{u2} / U_2$$

The ideal work input to the stage is given by :

$$H_{in\ id} = \zeta_i\ U_2^2$$

With the effect of slip factor the work input coefficient becomes :

$$\zeta_i = (C_{u2} / U_2)(SF).$$

And the total head input is :

$$H_{in} = \zeta\, U_2^2 = (C_{u2} / U_2)(SF)\, U_2^2 = C_{u2}(SF)\, U_2 \qquad (1.29)$$

1.1.6. Reaction and its effect on efficiency:

Reaction is defined as the ratio of the static head converted in the impeller to the total head produced by the stage.

$$R = (h_2 - h_0) / (h_{04} - h_{00})$$

where:

h_{04} = is the total enthalpy at stage outlet.

Neglecting the stage inlet kinetic energy (because it is small compared to that at the impeller outlet), the reaction becomes :

$$R = [(h_{04} - h_{00}) - C_2^2] / (h_{04} - h_{00})$$

Using the velocity triangles and taking into account that :

$\Phi = C_m / U$ where : Φ = flow coefficient.

Then

$$R = (1 - \Phi_2^2 \operatorname{cosec}^2 \beta_2) / 2 (1 - \Phi_2 \cot \beta_2) \qquad (1.30)$$

This reaction has an effect on the stage efficiency.

The isentropic efficiency is defined as (see figure 1.9.A) :

$$\eta_{is} = \Delta H_{4is} / \Delta H_{04} \qquad (1.30a)$$

The rotor efficiency is defined as:

$$\eta_{rot} = \Delta H_{2is} / \Delta H_{04} \qquad (1.30b)$$

The diffuser efficiency is defined as:

$$\eta = \Delta h_{24} / (C_2^{\,2} / 2) \qquad (1.30c)$$

From figure (1.9A) we can write

$$\Delta H_{4is} = \Delta h_{02} + \eta_d C_2^{\,2} / 2 - (1 - \eta_{rot}) \Delta H_{04}. \qquad (1.30d)$$

Assuming the line P_2 = constant and p_4 = constant are parallel then substtituting ΔH_{4is} in η_{is} we get :

$$\eta_{is} = (\Delta h_{02} / \Delta H_{04}) + (\eta_d C_2^{\,2} / 2 \Delta H_{04}) - (1 - \eta_{rot}) \qquad (1.30e)$$

Since:

$$R = \Delta h_{02} / \Delta H_{04} \qquad (1.30f)$$

And from figure (1.9A)we get:

$$C_2^{\,2} / 2\Delta H_{04} = (\Delta H_{04} - \Delta h_{02}) / \Delta H_{04} = (1 - R) \qquad (1.30g)$$

Substituting (1.30g) and (1.30f) into (1.30e) we get.

$$\eta_{is} = R + \eta_d (1 - R) - (1 - \eta_{Rot}) \qquad (1.31)$$

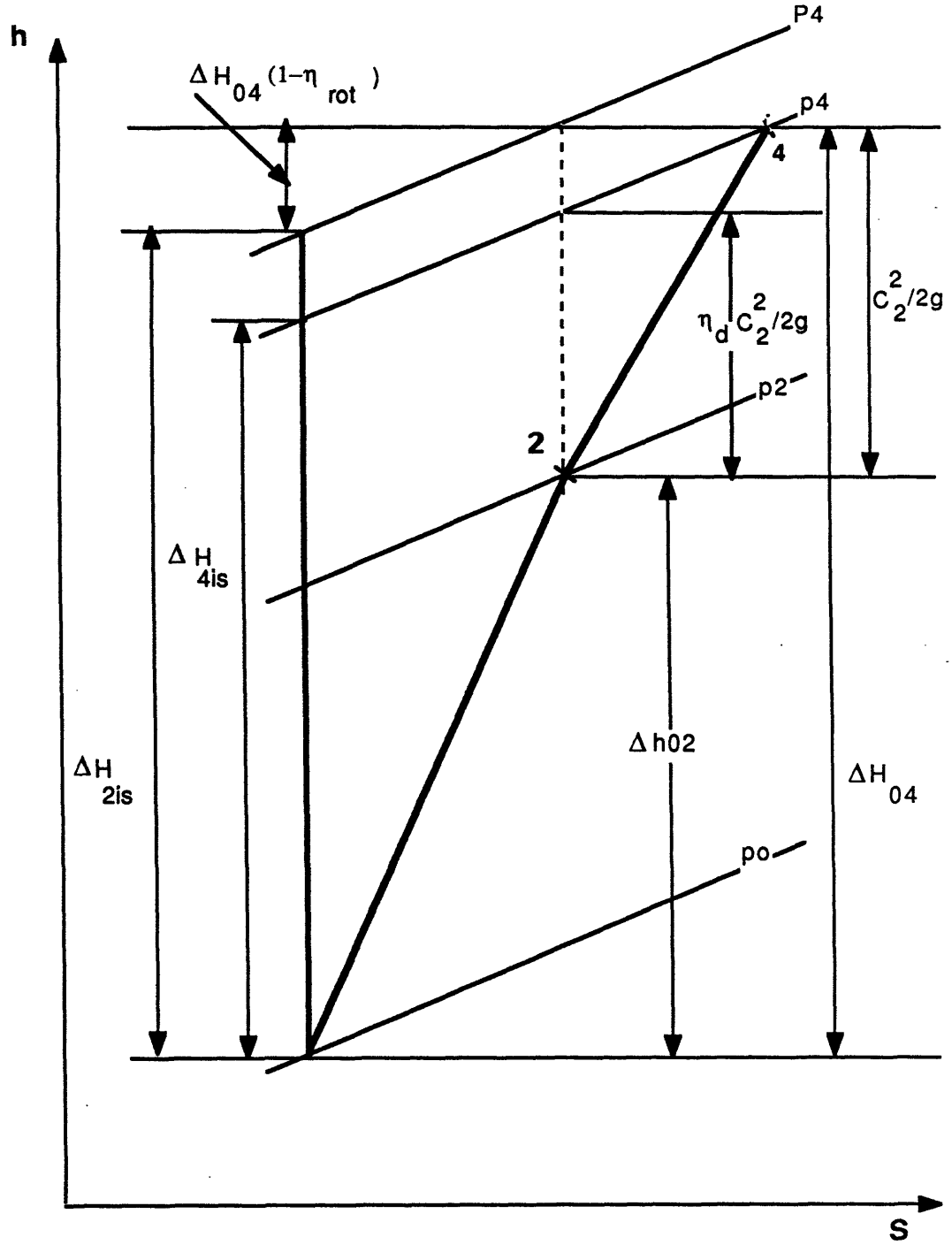

Fig. 1.9A. Irreversible centrifugal compressor stage with small inlt and outlet kinetic energy.

1.2. Radial Flow Turbines

1.2.1. Introduction:

The radial flow turbine was conceived about 170 years ago for the purpose of producing hydraulic power. Therefore it had a long history of development .

The radial outflow type was the first radial turbine to be developed in 1830. In 1847 *Francis* built the first radial inflow type of hydraulic turbine.

For best energy transfer it was found that the fluid should flow from a large radius to a smaller radius. Thus the best form for the radial turbine for compressible fluids would be that of an inward flow machine.

The majority of present day radial turbines both for compressible and incompressible flows are inward flow types.

1.2.2. Outward Flow Radial Turbines:

In this type of turbines the fluid enters the rotor in an axial direction and leaves it radially.

A flow path in reverse direction for a single stage turbine creates several problems, one of which is low specific work.

Ljungstrom conceived an outward-flow radial steam turbine which was found efficient and achieved a considerable reputation in Europe. This type of turbines has alternate rows of blades rotating in opposite directions, each driving a separate generator.

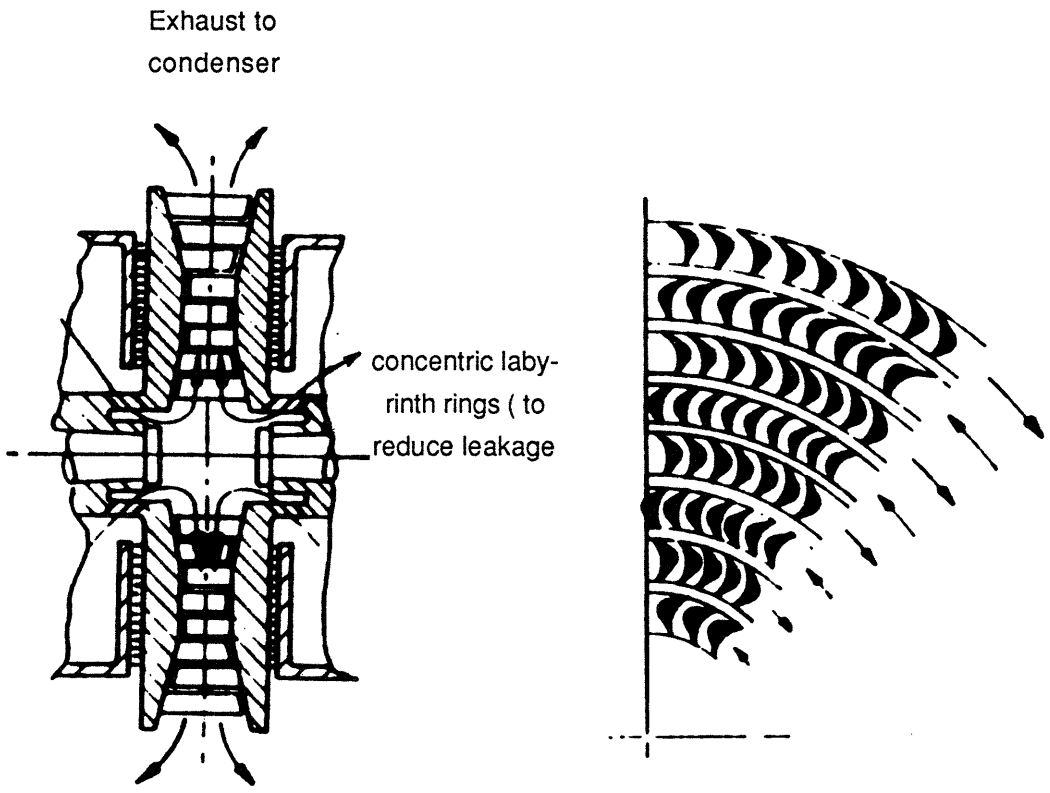

Fig. 1.10. Ljungstrom turbine .

1.2.3. Inward Flow Radial Turbines:

This type of machine has only become prominent recently, although its concept is not new. It is largely used in gas turbine power generation for small powers where its overall efficiency is better than the equivalent axial machine and where simplicity is prime requisite.

The singal stage inward flow radial turbine is very similar in principal and in appearance to the centrifugal compressor. Sometimes the inward flow radial turbine is called a *centripetal turbine* .

The radial configuration appears fundamentally less attractive than the axial when the resistance of material to the high temperatures is vital criterion. It is suggested that , for this reason, its selection for gas turbines cannot be justified from performance considerations alone, unless the variable area nozzle feature is utilized, or the specific speed involved is very low.

In connection with nozzles the inward flow radial turbines offer a distinct possibility of using variable nozzle vanes, a feature which is mechanically very difficult for the axial flow type of gas turbine. The use of variable nozzles is that they offer such an advantage in independent control of flow rate and energy transfer, a feature which is very desirable where a range of operating conditions is found.

Among the main advantages of the inward flow radial turbines of small size are :

1 - simple, rugged one piece rotor construction,

2 - cheaper manufacturing cost in comparison to the multi-blade axial flow type,

3 - have relatively higher efficiency for small gas flows compared to the axial flow type, for which very small aspect ratio blades may lead to a high percentage secondary flow loss.

Centripetal turbine is well suited because of its ability to handle large volume flows at high (rpm) .

The inlet angle for the IFR turbine is a major factor as for the centrifugal compressor the outlet angle is a major factor. The inlet vanes can be forward-curved or backward-curved or radial. The backward- curves allow the highest inlet whirl velocity and the forward-curved vanes allow the lowest whirl velocity. In practice, radial vanes are largely used because of stress considerations when used with hot gases, and because of manufacturing simplicity.

1.2.4. CANTILEVER IFR TURBINE:

The cantilever turbine is aerodynamically similar to an axial impulse turbine. Its design method is also similar to that of the axial impulse turbine.

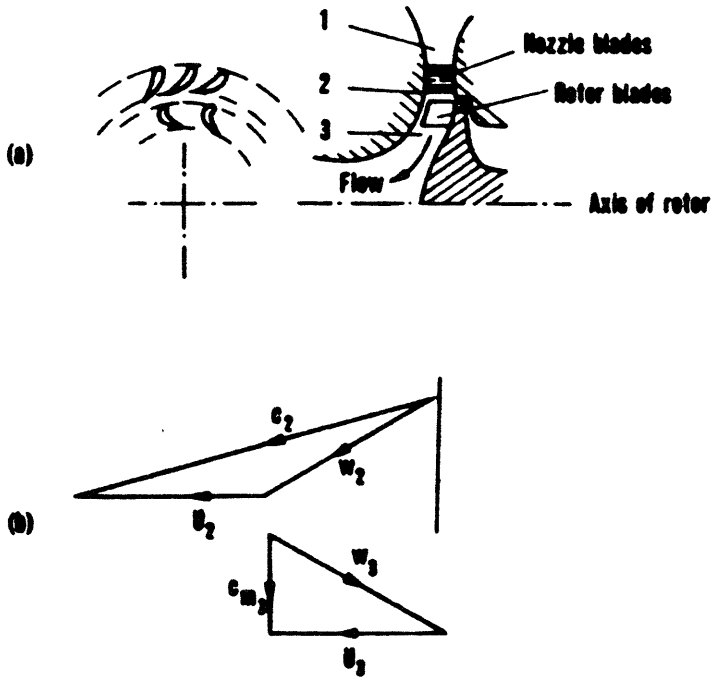

Fig. 1.11. Arrangement of cantilever turbine and velocity triangles at the design point.

1.2.5. The 90 Degree IFR Turbine:

The 90 degree IFR turbine is the preffered type of radial turbines to be used in gas turbine generation of small powers because of its higher structural strength than that of the cantilever turbine.
This turbine is called 90 degree IFR because its rotor blades extend from a radially inward inlet to an axial outlet .See figure (1.12).

As we defined previously , the rothalpy throughout the diffuser is constant

$$I_2 = I_3$$

Therefore:

$$h_{02\,rel} - 1/2\, U_2^2 = h_{03\,rel} - 1/2\, U_3^2 \qquad (1.32)$$

Since:

$$h_{0rel} = h + 1/2\, w^2 \qquad (1.33)$$

then

$$h_2 - h_3 = 1/2\,[\,(U_2^2 - U_3^2) - (w_2^2 - w_3^2)\,] \qquad (1.34)$$

From velocity triangles we obtain :

$$h_2 - h_3 = 1/2\, U_2^2\,[\,(1 - \cot^2 \alpha_2) + (r_3 / r_2)^2 \cot^2 \beta_3\,] \qquad (1.35)$$

Across the diffuser the total enthalpy is constant but the static enthalpy increases as a result of the velocity diffusion , and hence,

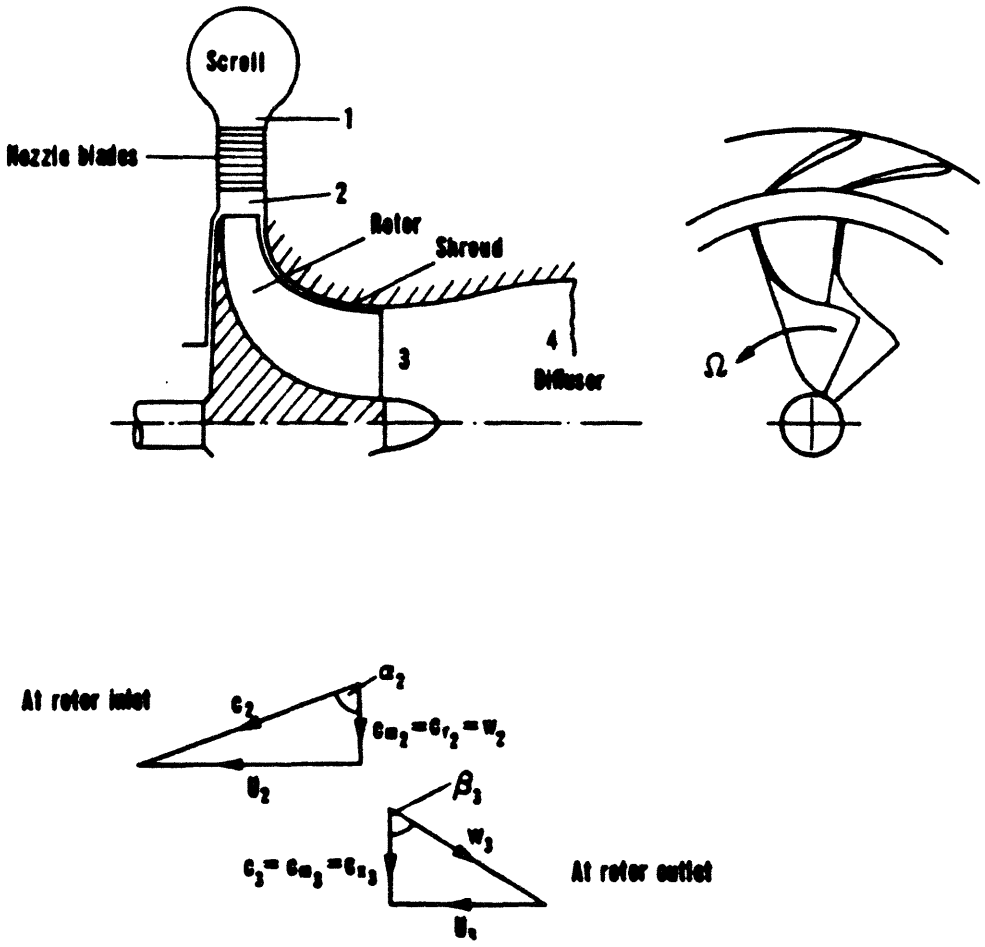

Fig. 1.12. Layout and velocity diagrams for a 90 deg IFR turbine at the nominal design point .

$$h_4 - h_3 = 1/2 \, (C_3^2 - C_4^2) \qquad (1.36)$$

The specific work done by the fluid on the rotor is :

$$\Delta W = 1/2 \, [\, U_2^2 - U_3^2 \,) - (\, w_2^2 - w_3^2 \,) + (\, C_2^2 - C_3^2 \,) \,] \qquad (1.37)$$

In turbomachinery design the temperature ratio is an important factor, it is given by :

$$\frac{T_3}{T_2} = 1 - \frac{1}{2} (\gamma - 1) \left(\frac{U_2}{a_2} \right)^2 \left[1 - \cot^2 \alpha_2 + \left(\frac{r_3}{r_2} \right)^2 \cot^2 \beta_3 \right] \qquad (1.38)$$

where :

$$a_2 = (\gamma R T)^{1/2}$$

The total to static efficiency is given by :

$$\eta_{ts} = (h_{01} - h_{03}) / (h_{01} - h_{3ss}) \qquad (1.39)$$

working this out we obtain :

$$\eta_{ts} = \left[1 + \frac{1}{2} \left\{ \xi_n \frac{T_3}{T_2} \operatorname{cosec}^2 \alpha_2 + \left(\frac{r_3}{r_2} \right)^2 (\xi_R \operatorname{cosec}^2 \beta_3 + \cot^2 \beta_3) \right\} \right]^{-1} \qquad (1.40)$$

where T3 / T2 is given by equation (1.38)

$$\xi_N = 1 / \psi_{N2} - 1$$

$$\psi_N = C_2 / C_{2S}$$

$$\xi_R = 1 / \psi_{R2} - 1$$

$$\psi_R = w_3 / w_{3s}$$

It was found experimentally that :

$$0.95 \leq \psi_N \leq 0.97$$

$$0.75 \leq \psi_R \leq 0.85$$

where :

ξ_N = Nozzle enthalpy loss coefficient,

ξ_R = Rotor enthalpy loss coefficient,

ψ_N = Nozzle velocity coefficient,

ψ_R = Rotor velocity coefficient.

The pressure ratio through the turbine (between nozzle inlet and rotor outlet) [16] is given by :

$$\left(\frac{p_{01}}{p_{03}}\right)^{\frac{\gamma-1}{\gamma}} = \frac{\left(\frac{C_3}{C_0}\right)^2 + \frac{\left[\frac{1}{2}(\gamma-1)M_3^2\eta_t\right]}{\left[1+\frac{1}{2}(\gamma-1)M_3^2\right]}}{\left(\frac{C_3}{C_0}\right)^2 - \frac{\left[\frac{1}{2}(\gamma-1)M_3^2(1-\eta_t)\right]}{\left[1+\frac{1}{2}(\gamma-1)M_3^2\right]}} \qquad (1.41)$$

Figure (2.4) [16] gives the variation of the pressure ratio as a function of $(C_3 / C_0)^2$ for mach numbers $M_3 = 1$ and $M_3 = 0.7$.

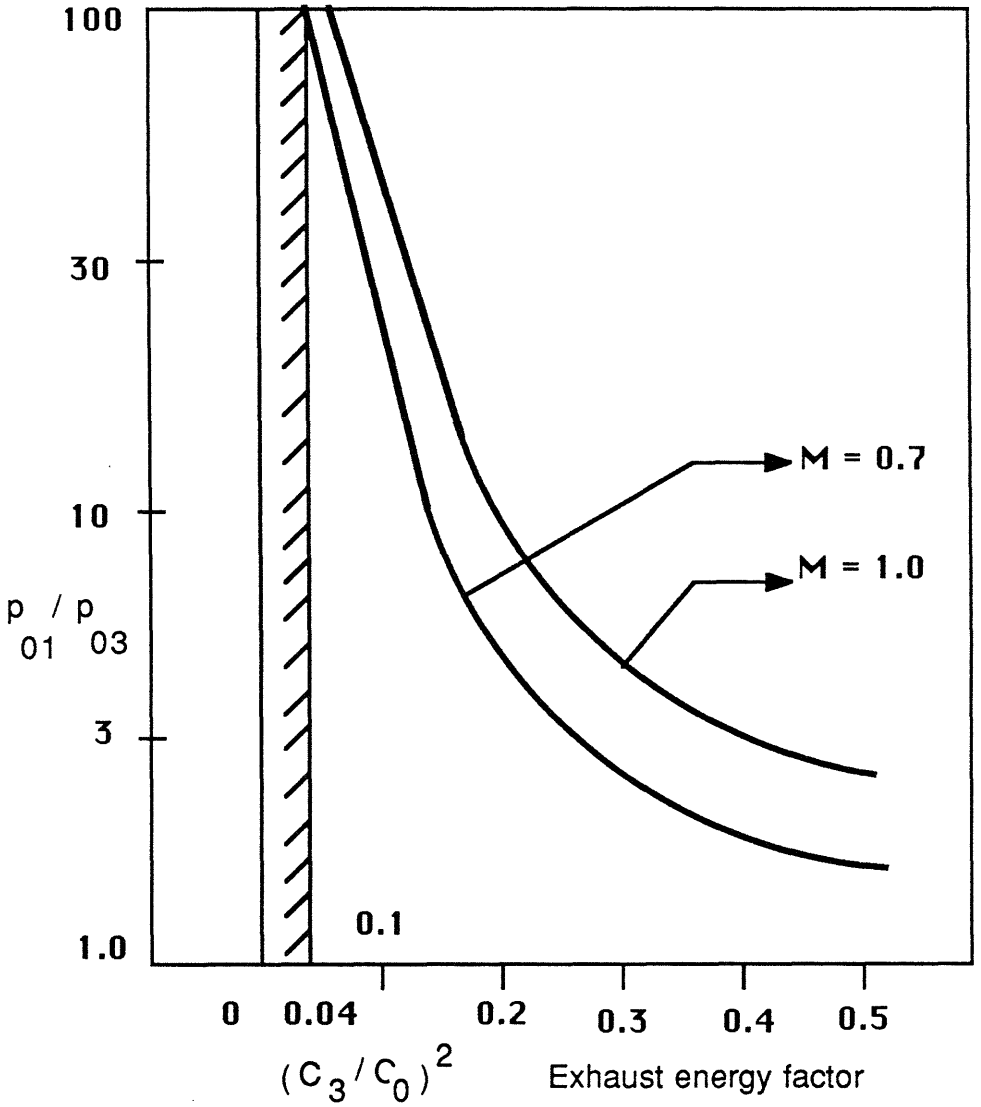

Fig. 1.13. Pressure ratio limit function.

1.2.6. Mnimum Number of Blades of a Radial Flow Turbine :

To avoid the phenomenon of reverse flow at the rotor tip, the criterion of optimizing the number of rotor blades is used. The minimum number of blades [14], Z_{min} , is given by :

$$Z_{min} = 2\pi \tan \alpha_2 \qquad (1.42)$$

Figure (2.5) shows the variation of Z_{min} with α_2.

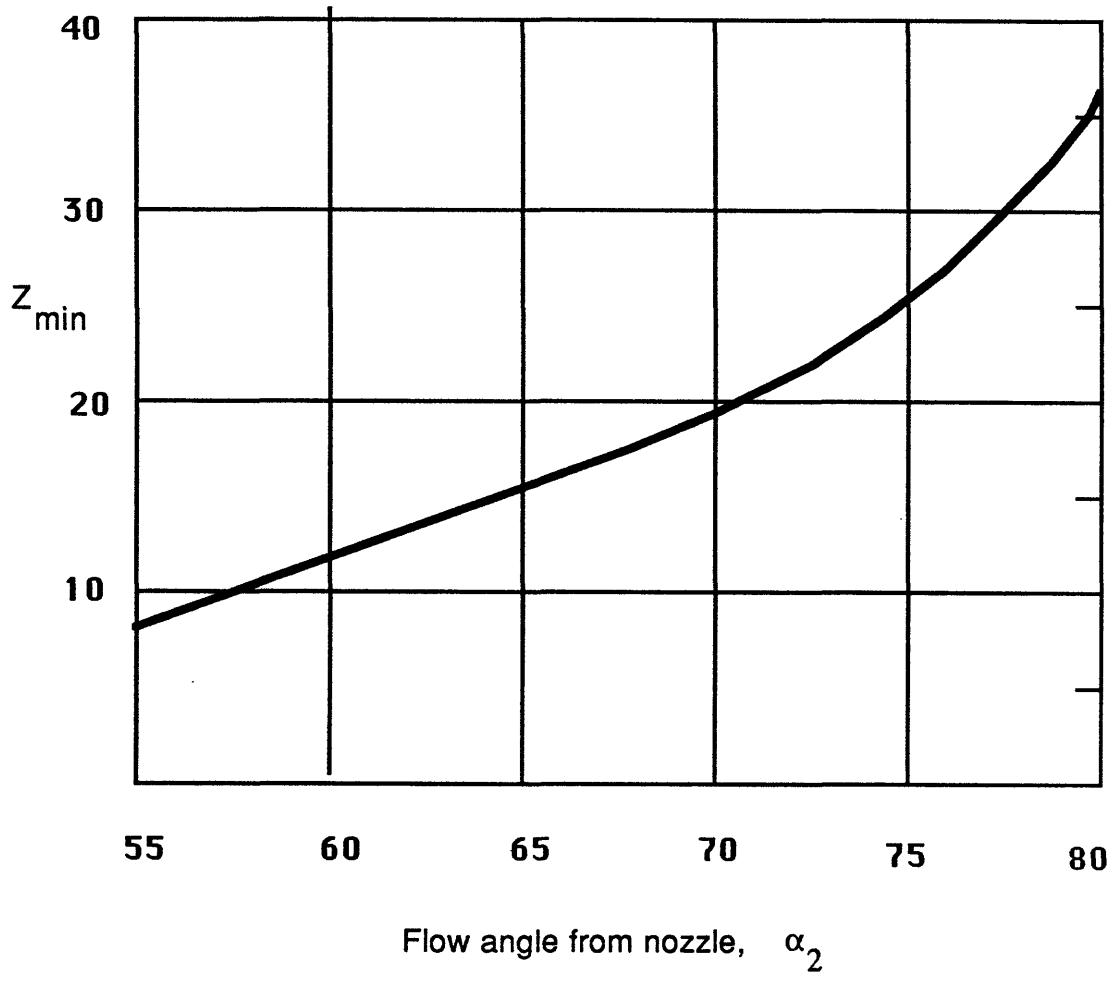

Fig. 1.14. Minimum blade number required to avoid flow reversal at rotor entry.

1.3. Axial Flow Compressors:

1.3.1. Introduction and Historic:

In the early 1880's there came an idea to Sir Charles Parsons to use an axial turbine and reverse it to obtain an axial flow compressor, but it was found that the efficiency was as low as 40% compared to that of the radial flow compressor which was much higher than that. An efficiency of the centrifugal compressor of 70 to 80% made them abandon the axial flow compressor. the low efficiency of the axial flow compressor was caused by the phenomenon of surge. It was until 1926 that any further development on axial flow compressors was undertaken when A. Griffith outlined the basic principles of his airfoil theory. After the use of this theory to the axial flow compressor the efficiency rised to a high number, about 90% for low pressure ratio stages. Axial flow machines are the most difficult type of turbomachines to be designed. It is possible by very careful design to attain higher performance than in the corresponding radial or mixed flow machines, it requires only relatively small deviations from the optimum conditions to reduce the performance disastrously.

1.3.2. Principal of Functioning of Axial Flow Compressors:

In the axial compressor work is done on the air through the medium of the rotor. It is converted partly into pressure by reduction of the relative velocity within the blade row, and partly into kinetic energy by an increase in the absolute velocity. This latter quantity is converted into pressure by

diffusion in the stator. The portion of the total energy input converted into pressure in the rotor defines the " *degree of reaction* ". If the whole of the energy input appears as kinetic energy, i.e. no pressure rise in the rotor, the design is reffered to as 0% reaction which is the impulse type. If all the pressure rise occurs in the rotor the design is said to be 100% reaction. In practice, the 50% reaction type of axial machine is commonly used because it simplifies the method of design of the machine and the velocity triangle is symmetric.

1.4. Axial Flow Turbines:

1.4.1. Introduction and Historic:

For small powers radial turbines are widely used, but they are not so suitable for the high temperature environment of a gas turbine engine. For all but the lowest powers the axial flow turbine is more efficient . The axial flow gas turbine is not new in concept, it only became of major importance in the 20 th century, because its successful use had to wait for the development of efficient compressors and of materials of high strength at elevated temperatures. The axial flow turbine usually has only a few stages where the axial flow compressor has many stages so that the phenomenon of surge can be avoided , whereas the axial turbine does not have that problem of surge.The design method of an axial turbine consists of designing one stage and assuming that all its stages are symmetric, if the turbine has more than one stage, one can generalize for the rest of the stages.

1.4.2. Principal of Functioning and Theoretical Analysis:

The principal of work of the axial turbine stage is that the gas entering the row of the stator blades with a static pressure and temperature p_1 , T_1 , and a velocity C_1 is expanded to p_2, T_2, and leaves with an increased velocity C_2 and at angle α_2 . After being deflected , and usually further expanded, in the rotor blade passages the gas leaves at p_3 , T_3 , and relative velocity w_3 at angle β_3 . Figure (1.15) shows the velocity triangles at inlet and outlet of each blade row.

Assuming adiabatic flow, the work done on the rotor by unit mass of fluid equals the stagnation enthalpy drop incurred by the fluid passing through the stage.

$$\Delta W = h_{01} - h_{03}. \qquad (1.43)$$

The most important factor in the design of turbomachinery is the efficiency. Therefore we give the expressions of the different efficiencies.
The total to total efficiency is defined as :

η_{tt} = (Actual work output) / (ideal work output when operating to same back pressure)

$$\eta_{tt} = (h_{01} - h_{03}) / (h_{01} - h_{03ss}) \qquad (1.44)$$

$$\eta_{tt} = (h_{01} - h_{03}) / (h_{01} - h_{03ss}) \qquad (1.44)$$

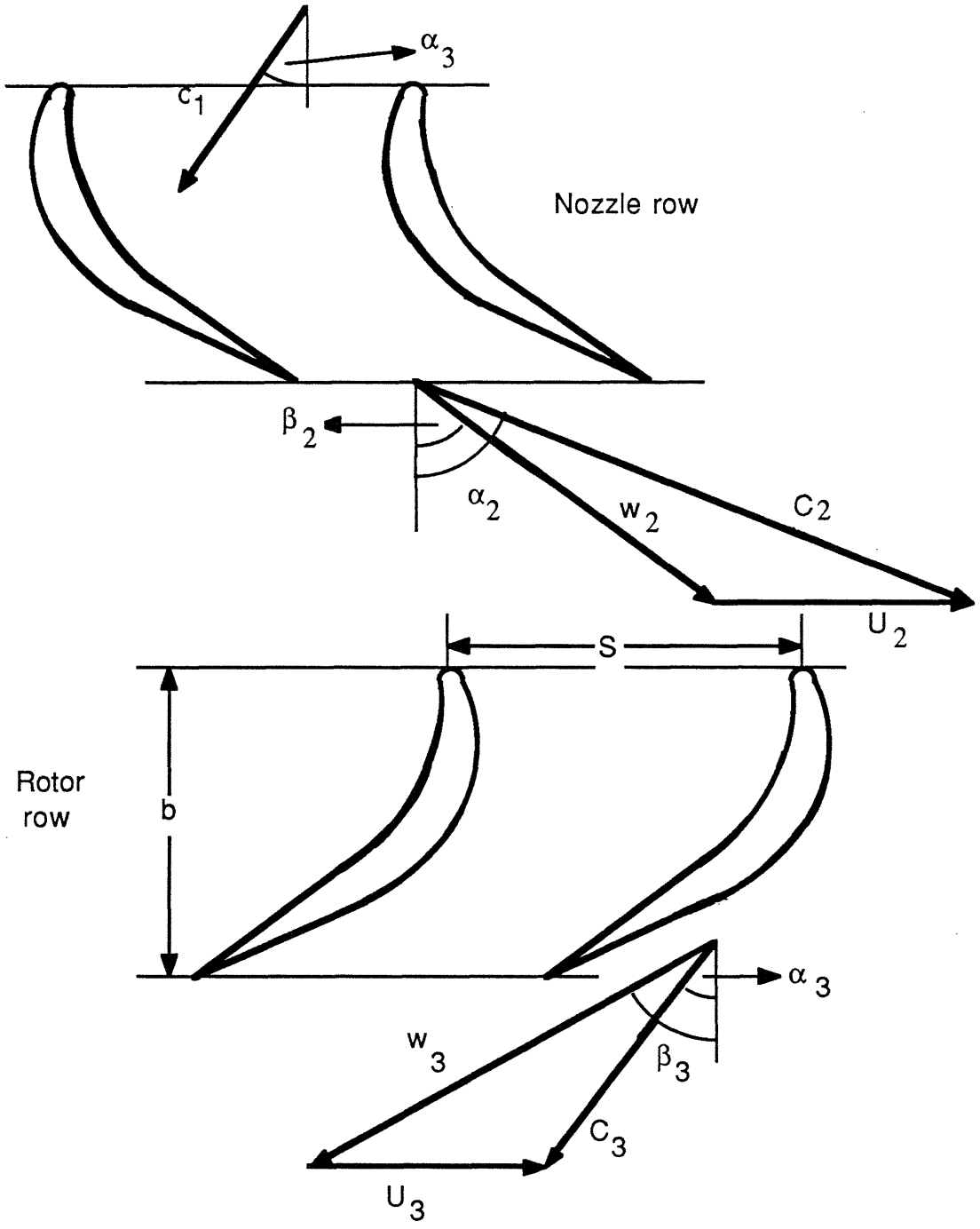

Fig. 1.15. Axial turbine stage velocity diagram.

For a normal stage :

$$C_1 = C_3$$

$$\alpha_1 = \alpha_3$$

Then we can write :

$$\eta_{tt} = (h_1 - h_3) / [\, (h_1 - h_3) + (h_3 - h_{3s}) + (h_{3s} - h_{3ss}) \,] \qquad (1.45)$$

Since :

$$h_{3s} - h_{3ss} = (T_3 / T_2)\,(h_2 - h_{2s}) \qquad (1.46)$$

$$h_2 - h_{2s} = 1/2\, C_2^2\, \xi_N \qquad (1.47)$$

$$h_3 - h_{3s} = 1/2\, w_3^2\, \xi_R. \qquad (1.48)$$

Substituting the three latter equations into equation (1.45) we obtain :

$$\eta_{tt} = \left[1 + \frac{\xi_R\, w_3^2 + \xi_N\, C_2^2\, \frac{T_3}{T_2}}{2\,(h_1 - h_3)} \right]^{-1} \qquad (1.49)$$

The total to static efficiency is defined as :

$$\eta_{ts} = (h_{01} - h_{03}) / (h_{01} - h_{3ss}) \qquad (1.50)$$

Working equ. (1.50) out and using (1.47) and (1.48) we get :

$$\eta_{ts} = [1 + \{ \xi_R w_3^2 + \xi_N C_2^2 (T_3 / T_2) + C_1^2 \} / 2 (h_1 - h_3)]^{-1} \qquad (1.51)$$

Axial flow turbines can be classified using the degree of reaction, which is defined as the ratio of static enthalpy drop in the rotor to the static enthalpy drop in the stage .

$$R = (h_2 - h_3) / (h_1 - h_3) \qquad (1.52)$$

Using velocity triangles the expression of the reaction becomes:

$$R = 1 + \Delta W / 2 U^2 - C_{y2} / U$$

The effect of the degree of reaction on the total to total efficiency is not large. η_{tt} is decreased when the stage loading factor is increased . Therefore for a high total to total efficiency it is necessary to use the highest possible blade speed consistent with blade stress limitation, in other words reduce the loading coefficient . The effect of the degree of reaction on the total to static efficiency for different values of the blade loading coefficient $\Delta W / U^2$ is illustrated by the figure bellow.

η_{ts} is expressed as a function of the degree of reaction :

$$\eta_{ts} = [1 + \phi^2 (1 + \tan^2 \alpha_3) / 4 (\phi \tan \alpha_3 + 1 - R)]^{-1}$$

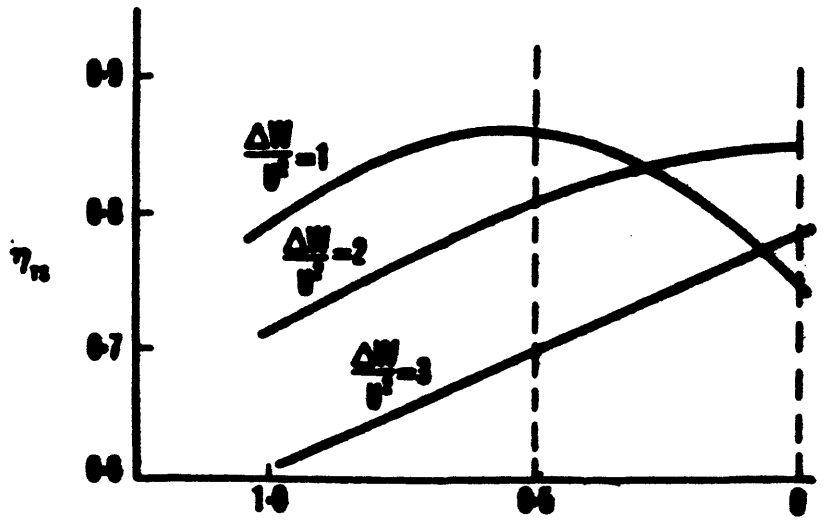

Fig. 1.16. Influence of reaction on total-to-static efficiency with fixed values of stage loading coefficient .

CHAPTER 2

PROBLEM FORMULATION

2.1. A 2 to 15 kwe power generation system

A 10 kwe net output radial outflow compressor was investigated and designed by NASA Lewis Research Center. This system was designed to develop a wide range of power from 2 to 15 kwe.

The research consists of a 4.25 IN diameter compressor wheel and shaft mounted on bearings and the associated mounting hardware. Fig.(2.1) shows the scheme of the brayton rotating unit compressor wheel.

The compressor design conditions resulting from the analysis are as follows

The system uses He-Xe mixture at equivalent molecular weight of 83.9 as working fluid. The compressor inlet pressure and temperature are, 13.5 psia and 80 ^{o}F . The pressure ratio is 1.90. AT the low power level (2 kwe) the pressure is high enough to provide satisfactory bearing operation . At the high level (15 kwe), the pressure is not so high to in large alternator windage losses.

The rotational speed is restricted to that which would produce a multiple of 400 Hz from the four pole alternator to minimize the windage losses in the alternator. It is also chosen for maximum efficiency. It is clearly seen on fig. (2.2) that the maximum efficiency is at a rotational speed of 36,000 rpm.

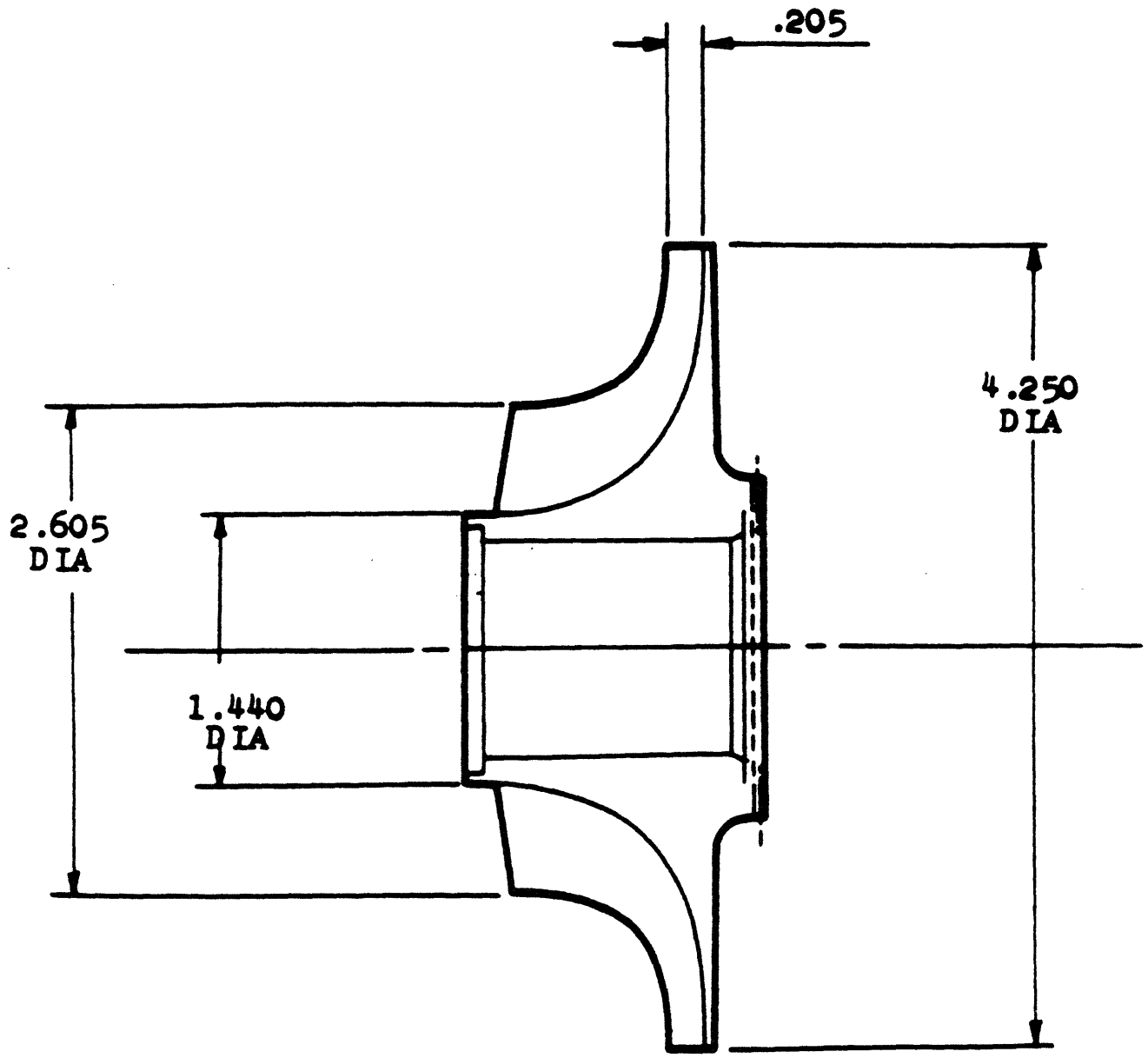

Fig. 2.1. Brayton rotating unit compressor wheel

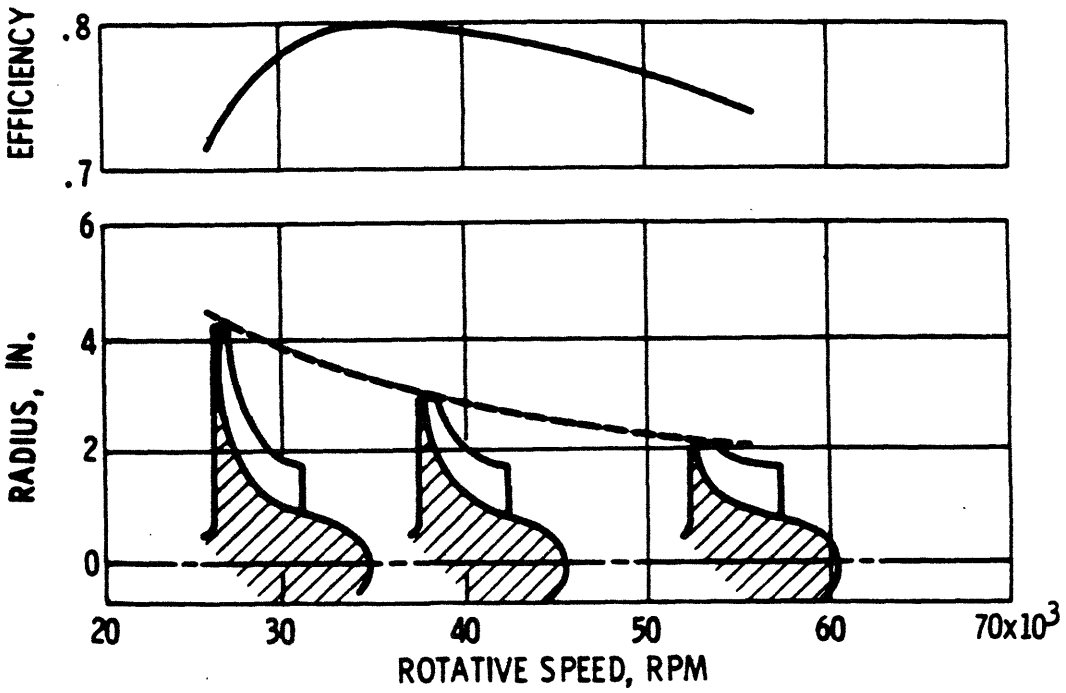

Fig. 2.2. Centrifugal compressor efficiency - geometry relation.

The compressor efficiency at scroll exit was about 0.80 which is a good efficiency for such a small machine where clearance loss is a major problem.

For the turbine, the radial inflow type was selected. It was found that this type of turbine offers better design conditions than those of the axial type turbine.

Again , the working fluid is a mixture of He-Xe at equivalent molecular weight of 83.9 at weight flow of 0.34 kg / sec.

The turbine total to total pressure ratio is 1.74, its specific speed was calculated based on the given conditions :

Maximum cycle temperature	T_{max} = 1150 ^{o}k
Specific heat	Cp = 0.248 kJ / kg.^{o}k
Actual specific work	Δh = 50.404 kJ / kg
Turbine temperature ratio :	τ_t = 0.822
The specific speed is:	Ns = 76.20

The size of the turbine is illustrated in figure (2 . 3).

At turbine inlet temperature of 1150 ^{o}k and power output of 10.5 kwe, the total turbine efficiency was 0.8858 . The radial inflow turbine designed for the 10 kwe output power offers the system an overall efficiency of the order of 0.30 and can work at an output power up to 15 kwe. The variation of efficiency with net output power is shown on figure (2.4). If we compare this efficiency to that of the two-stage-axial turbine whose efficiency was 0.847 [39] designed for a Brayton rotating unit , we will notice clearly why radial type turbine was chosen.

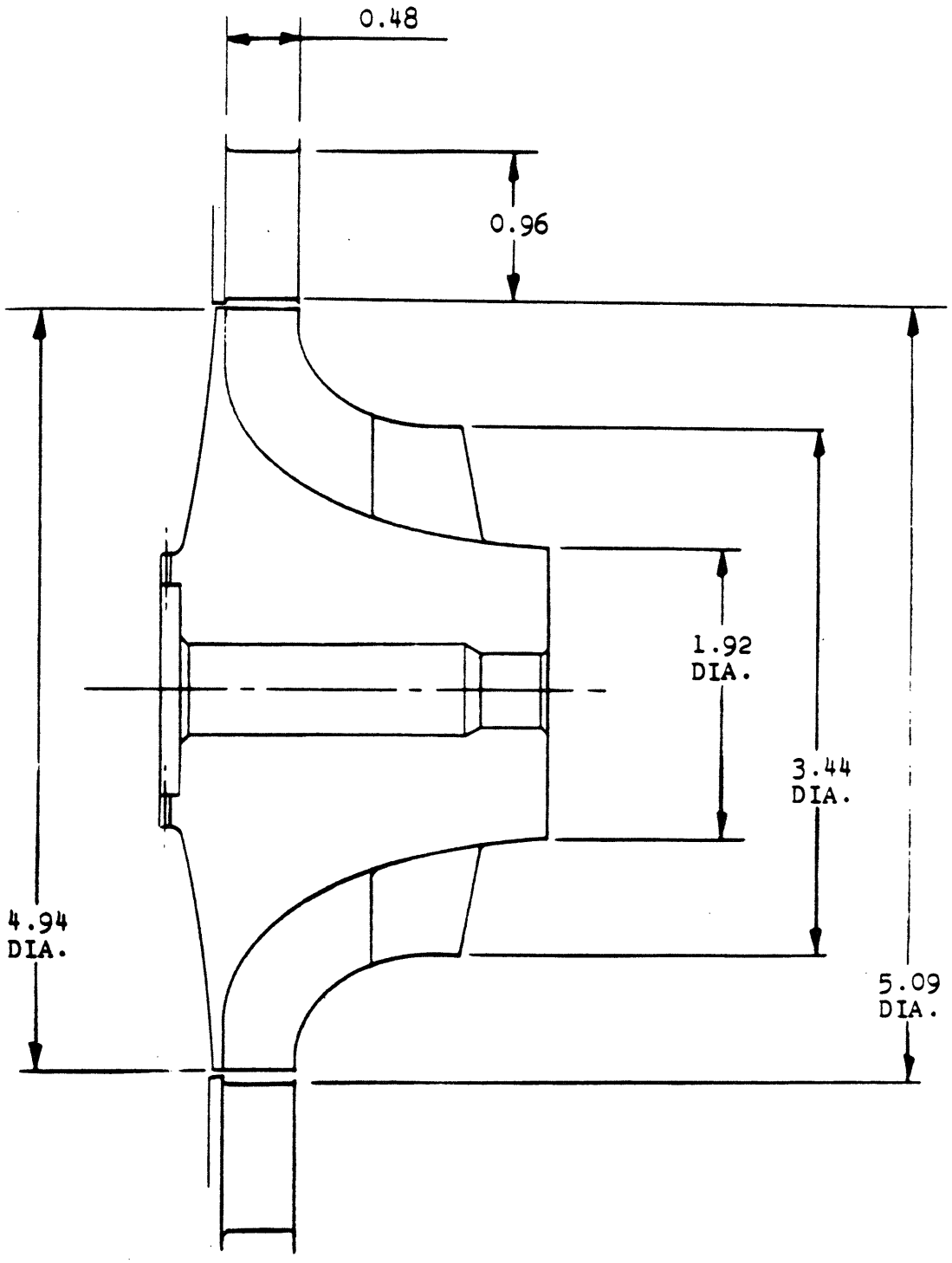

Fig. 2.3. Brayton Rotating Unit Turbine Design.

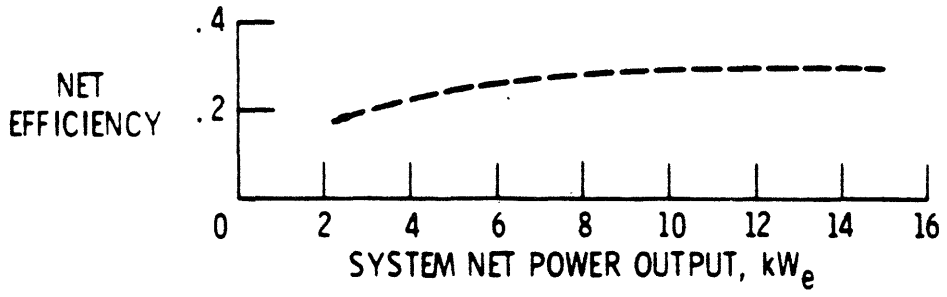

Fig. 2.4. Variation of efficiency with the net output power.

A two - stage axial turbine was also designed to drive an alternator for a 10 kw shaft output space power system. The stage total efficiency was 0.847 and the two - stage total efficiency was 0.850 which is based on total efficiencies of 0. 847 for first and second stages. The turbine overall efficiency was 0.843. All these efficiency values were obtained at design point. Comparing the two efficiencies of the two turbines, we will find clearly that the radial turbine efficiency is 4.3 % higher than that of the two-stage axial turbine designed; Therefore the radial turbine the best suited for this range of power.

2.2. A 15 to 80 kwe power generation system:

The ability of a closed Brayton cycle power generation system to operate with good performance over a range of power levels and cycle conditions permits a single developed system to be used for a variety of applications and missions.

The missions may need to operate at different power levels and may require selection of different cycle operating conditions. A 15 to 80 kwe reactor Brayton power system is developed by NASA - Lewis, the system operates at a maximum cycle temperature (turbine inlet temperature) of the order of 1150 ^{o}K . The turbine inlet temperature is a very important parameter, the higher the temperature is , the higher the system efficiency is. It is also very important for the specific radiator area which reduces the weight of the whole system. It is very clear on the figure below that the higher the maximum cycle temperature is, the lower the specific radiator area is.

The compressor pressure ratio was 1.80 and the turbine pressure ratio was 1.73 .

This power generation system used a centrifugal compressor and radial turbine because of their high efficiencies and low energy losses compared to the axial type machines, and because of their manufacturing simplicity and compactness.

The compressor efficiency at design point was 0.83 and the turbine efficiency was 0.90.

The system used He-Xe mixture as a cycle working fluid at equivalent molecular weight of 83.9. It is to be noticed that the higher the equivalent molecular weight is the lower the number of turbine stages is.

Figure (2-6) below explains that increasing the working fluid equivalent weight decreases the number of stages to less than one stage.

With working fluid equivalent weight of 83.9 , a turbine turning at 36,000 rpm would have less stress than that of the same type of turbine but having a working fluid of equivalent molecular weight 40.

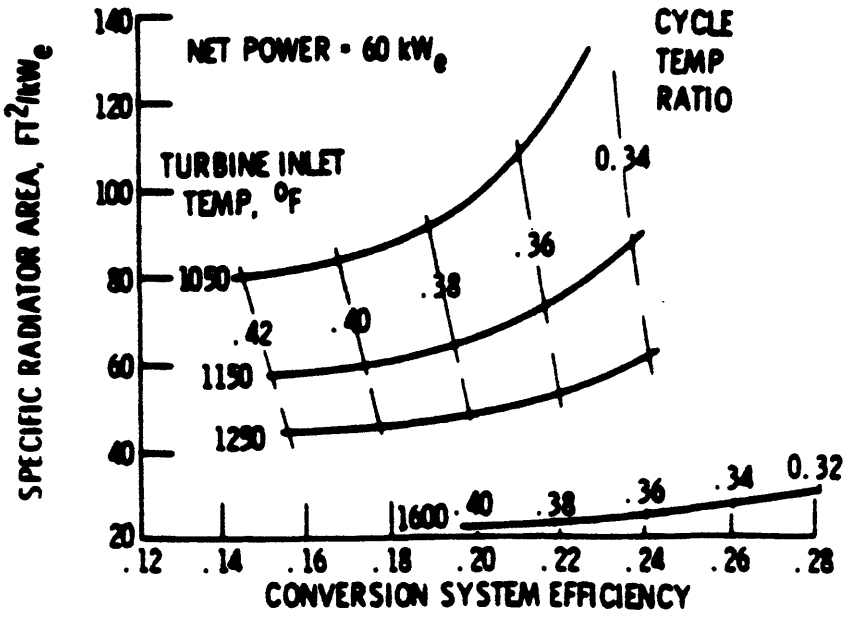

Fig. 2.4. Effect of turbine inlet temperature on system performance characteristics

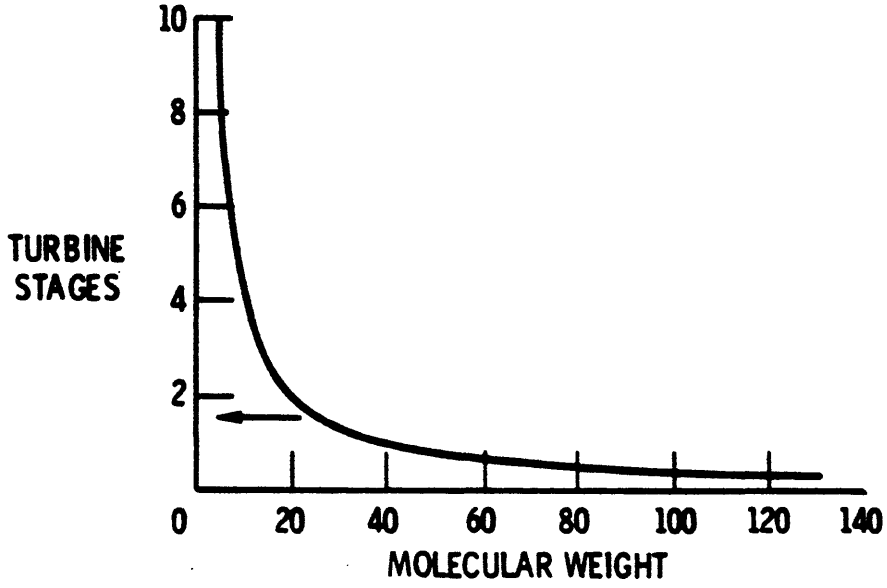

Fig. 2.6. Effect of molecular weight on turbomachinery.

The system has an overall efficiency depending on the power level at which it is working . It is low for low output powers and increases for increasing power output.

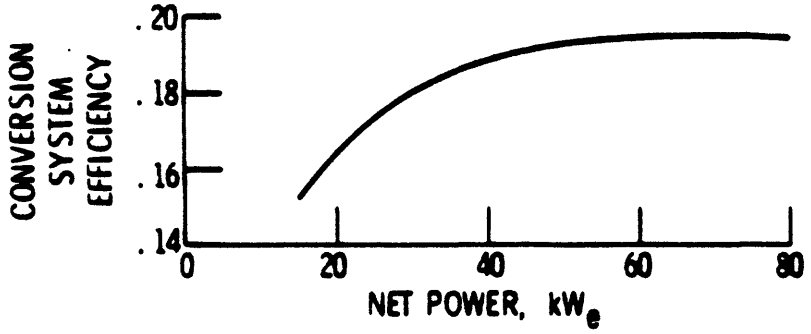

Fig. 2.6. Variation of overall efficiency with net power.

2.3. Design of a 160 kwe power generation system:

Component analyses were performed for both axial and centrifugal compressors, and comparison between the two configurations was made.

A notation was given to the type of machine designed. The first two digits denote the rotational speed in kilorpm, the third digit refers to the type of compressor, A denotes the axial configuration, R denotes the radial configuration, G means that the system has gas bearings, and M means that the system uses mist-lubricated ball bearing. For all configurations the working fluid is a mixture of He-Xe of equivalent molecular weight 83.9.

The 24 RG is a radial compressor turning on gas bearings at rotational speed of 24,000 rpm. The gas enters the compressor at 240 ^{o}F and 55 psia and leaves it at 500 ^{o}F and 105 psia. The inlet and the exit tip diameters are 7.25 and 10.36 IN respectively. The total efficiency at 160 kwe is 0.862 and at 40 kwe the total efficiency is 0.860.

The compressor wheel alone weighs 10 pounds, and the total rotor (including the compressor, the alternator rotor, the turbine, and the subshafts) weighs 152 pounds.

The 24 AG configuration is an axial compressor of 7 stages turning at a rotational speed of 24,000 rpm on gas bearings. The compressor has a total efficiency of 0.866 at full power (design point) and 0.837 at 40 kwe

which is much lower than that of the corresponding radial compressor. Its inlet tip diameter is 6.67 IN and it weighs 20 lbs. The total rotor weighs 165 pounds.

The 36 AM configuration is an axial compressor turning at a rotational speed of 36,000 rpm on mist-lubricated ball bearings. The compressor has a total efficiency 0.862 at 160 kwe and 0.840 at 40 kwe. The compressor eight is 6 lbs and the total rotor weighs 119 pounds.

The 36 RM configuration is centrifugal compressor turning at rotational speed 36,000 rpm on mist-lubricated ball bearings. The compressor weighs only 2 pounds. and the total rotor weight is only 112 pounds. The compressor efficiency at design point is 0.862 and at 40 kwe power it is 0.860 which is higher than that of the corresponding axial compressor. This configuration has the lowest weight compared to all the previous configurations.

From a comparison of the mechanical designs it is concluded in reference [19] that the 24 RG , which is a radial compressor turning at a rotational speed of 24,000 rpm on gas bearings , with radial inflow turbine provides the most suitable unit for the design conditions.

The Lundell alternator [41] was chosen for this turbo-alternator-compressor system. This type of alternator runs at high speeds up to 36,000 rpm. Its principle of design consists of two concentric cylinders.

At high speeds the windage losses in the alternator become high and result in significant heating of the electric generator. The windage losses in watts are given by the expression :

$$W = T\omega$$

Where :

$$\omega = U / R = 2\pi N$$

T : is the torque due to viscous drag defined as

$$T = F R$$

Where :

F : is the frictional force given by:

$$F = \lambda (2\pi R L) / [1/2 \ \rho U^2]$$

λ : is the drag coefficient given by the expression :

$$\lambda = T / (\rho \pi \omega^2 R^4 L)$$

with

T : the measured torque.

At rotational speed of 36,000 rpm the windage losses are 4.7 kw, and at 24,000 rpm they are only 1.5 kw , which is much lower than the first one. Figure (2.7) below shows the windage losses plotted vs. the rotational speed.

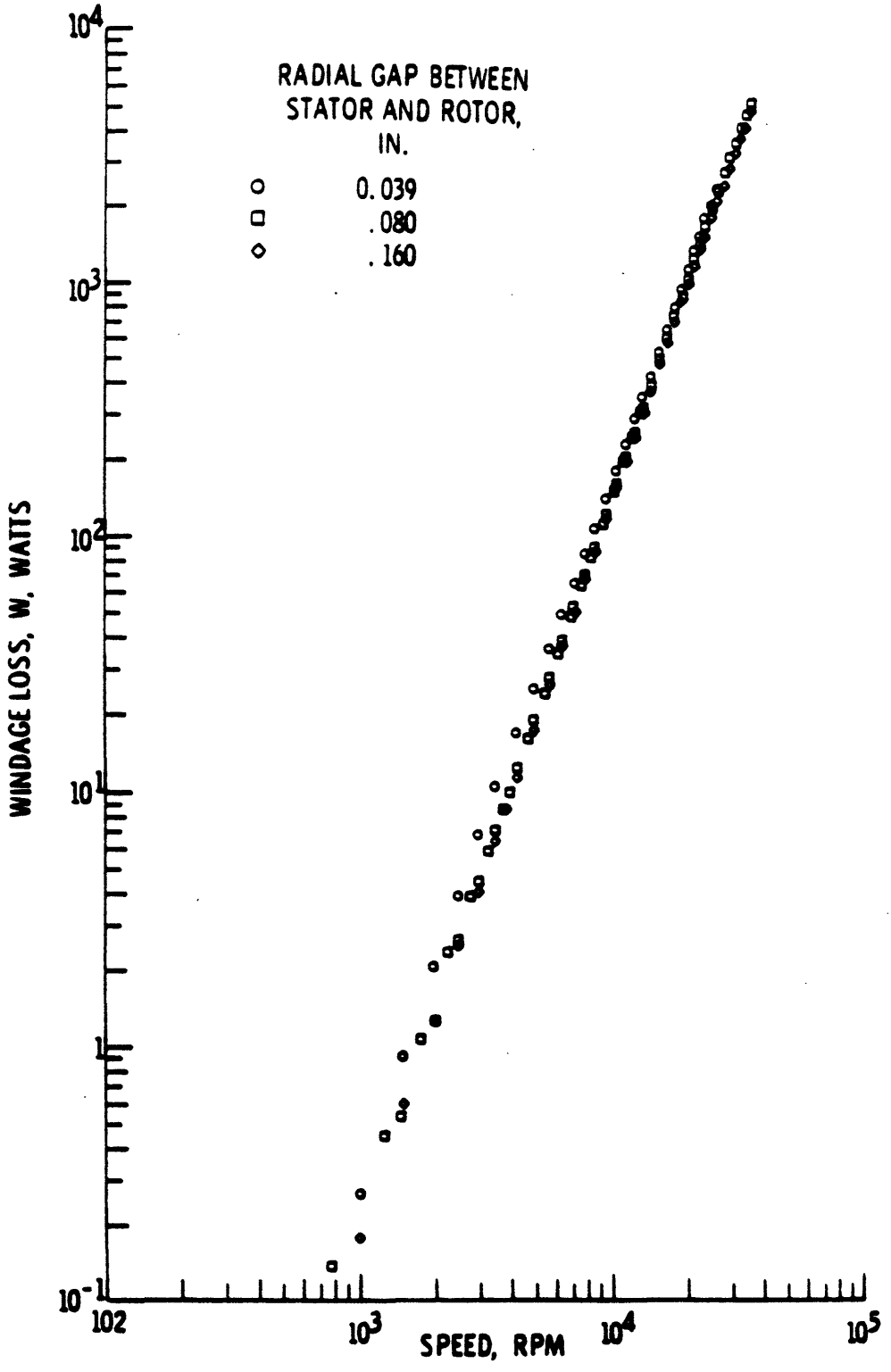

Fig. 2.7. Windage power loss for a Lundell-type rotor.

For all configurations the turbine was chosen radial because it is still better than the axial type at this level of power. The turbine weighs only 8 pounds for a 36,000 rpm, and 25 pounds for the 24,000 rpm configuration. Its efficiency was very high, It was 0.916 at design point [19].

The system overall efficiency is 28.4 % at 160 kwe and 24.7 % at 40 kwe for a turbine inlet temperature of 1600 ^{o}F.

2.4. Specific Speed :

2.4.1. Similarity Relations and Design Criteria of Turbines :

Similarity considerations show that two characteristic velocity ratios are needed to describe the characteristics of turbomachines. These velocity ratios can either be the flow factor and turbine-velocity ratio or equivalent values. Parameters which contain the rotational speed and rotor diameter would be desirable terms for equivalent values. These values are provided in the form of specific speed N_S and specific diameter D_S .

Specific speed N_S is a parameter of great importance in selecting the type of machine required for a given duty. This parameter is found proportional to the volume flow rate Q, the rotational speed N and the head H. Since for a given turbine the power and the rotational speed are normally specified, then it becomes of good use to consider this parameter which is sometimes called the shape number.

This parameter represents the rotational speed of a turbine, handles a volume flow of unity and expands a head of unity. Another important parameter in the selection of the type of machines required for a given duty is the specific diameter D_S.

H : Is the head.

h : Is the enthalpy

where:

$$g\,H = h = Cp\,T_{tmax}\,(1 - \tau_t) \qquad (2.1.a)$$

Q_3 : is the volume flow rate at the rotor exit.

The specific diameter It is defined as the diameter of a turbine which handles a volume flow Q_3 of unity at exit and expands a head of unity.

Ns and Ds are obtained as follows :

The volume flow Q_3 is proportional to the velocity and the area of passage. The area is proportional to (D^2). The velocity is proportional to ω (angular velocity) and the diameter is proportional to N (rotational speed). Then :

$$Q_3 \;\alpha\; ND^3 \qquad (2.1.b)$$

H is proportional to the square of the velocity which is proportional to ND. Then :

$$H \;\alpha\; N^2D^2. \qquad (2.1.c)$$

Taking a standard turbine we get :

$$Q_{3S} \;\alpha\; Ns\,Ds^3 \qquad (2.1.d)$$

$$H_s \;\alpha\; Ns^2Ds^2 \qquad (2.1.e)$$

$$Q_3 / Q_{3\text{-}S} = ND / NsDs \qquad (2.1.f)$$

$$H / H_S = N^2D^2 / Ns^2 Ds^2 \qquad (2.1.g)$$

Solving equations (2.1.f) and (2.1.g) for :

$$H_S = Q_{3\text{-}S} = 1$$

we get :

$$Ns = N Q_3^{1/2} / H^{3/4} \qquad (2.1)$$

where,

$$Ds = D H^{1/4} / Q_3^{1/2} \qquad (2.2)$$

The dimensionless specific speed and specific diameter are defined as follows:

$$n_s = Q_3^{1/2} \omega / (g.H)^{3/4} \qquad (2.3.a)$$

$$\omega = \pi N / 30$$

$$ds = D (g.H)^{1/4} / Q_3^{1/2} \qquad (2.3.b)$$

The enthalpy transformed into rotative power (H_R) is given by :

$$H_R = \frac{F u}{\dot{m}}$$

Where F is the force exerted by the velocity vectors on the rotor.

$$F = \dot{m} (C_{u-2} + C_{u-3}) \qquad (2.4)$$

C_u denotes the peripheral Component of the absolute velocity while 2 and 3 denote the inlet and the outlet of the rotor, respectively.

C_{u-2} and C_{u-3} can be expressed by :

$$C_{u-2} = C_2 \cos \alpha_2 = \psi_N \sqrt{1 - R}\, C_o \cos \alpha_2 \qquad (2.5)$$

where :

R : The degree of reaction

C_o : The spouting velocity (the velocity obtained when the total turbine pressure ratio is ideally expanded into Kinetic Energy).

Ψ_N : The velocity coefficient of the nozzle. It expresses the ratio of the actual velocity and the theoretical velocity. The theoretical velocity refers to the velocity which would be obtained when no losses have to be considered in the flow passage.

Considering this velocity coefficient in our calculations means that we consider the losses that occur in the flow passages in the nozzle. Experimental investigations show that the nozzle velocity coefficient can for most cases be considered constant and takes the numerical value.

$$\psi_N = 0.96$$

The rotor outlet peripheral velocity can be expressed by :

$$C_{u\text{-}3} = w_{u\text{-}3} - u \qquad (2.6)$$

$$C_{u-3} = C_o \psi_R \cos\beta_3 \sqrt{R + (1-\rho)\psi_N^2 - 2\psi_N \cos\alpha_2 (1-R)^{1/2} \frac{u}{C_o} + \left(\frac{u}{C_o}\right)^2} - u$$

ψ_R : denotes the velocity coefficient in the rotor. It also takes into account all the losses that can occur in the rotor, the following expression gives this coefficient :

$$\psi_R = \left\{ 1 - \frac{\cot\alpha_2}{30} + \frac{N_s D_s \sqrt{1-2\frac{h}{D} + 2\left(\frac{h}{D}\right)^2}}{4620\, \psi_N \sin\alpha_2} \right\}$$

$$x \left\{ 1 - \frac{0.24 \cos\beta_2 \frac{a^*}{D}}{\frac{h}{D}} \right\}$$

These two coefficients are considered in the determination of the efficiency of both axial and radial turbines. The efficiencies were obtained as functions of the specific speed Ns and the specific diameter Ds.

Reference [31] gives plots of Ns -Ds diagrams which were used here to plot the efficiencies of the radial and axial turbines verses specific speed Ns.

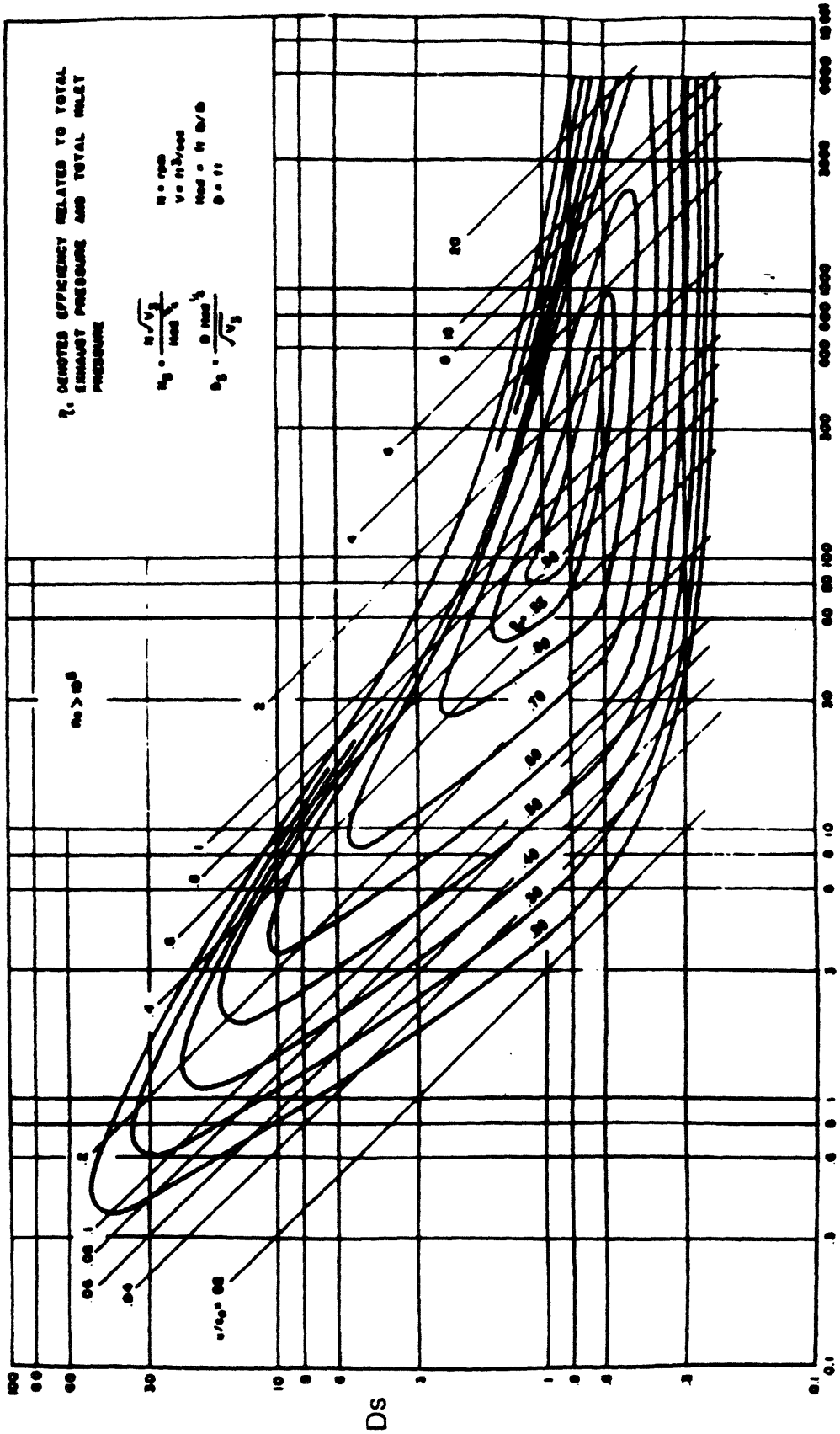

Fig 2.8. Ns-Ds diagram for single-disk turbines showing total efficiency.

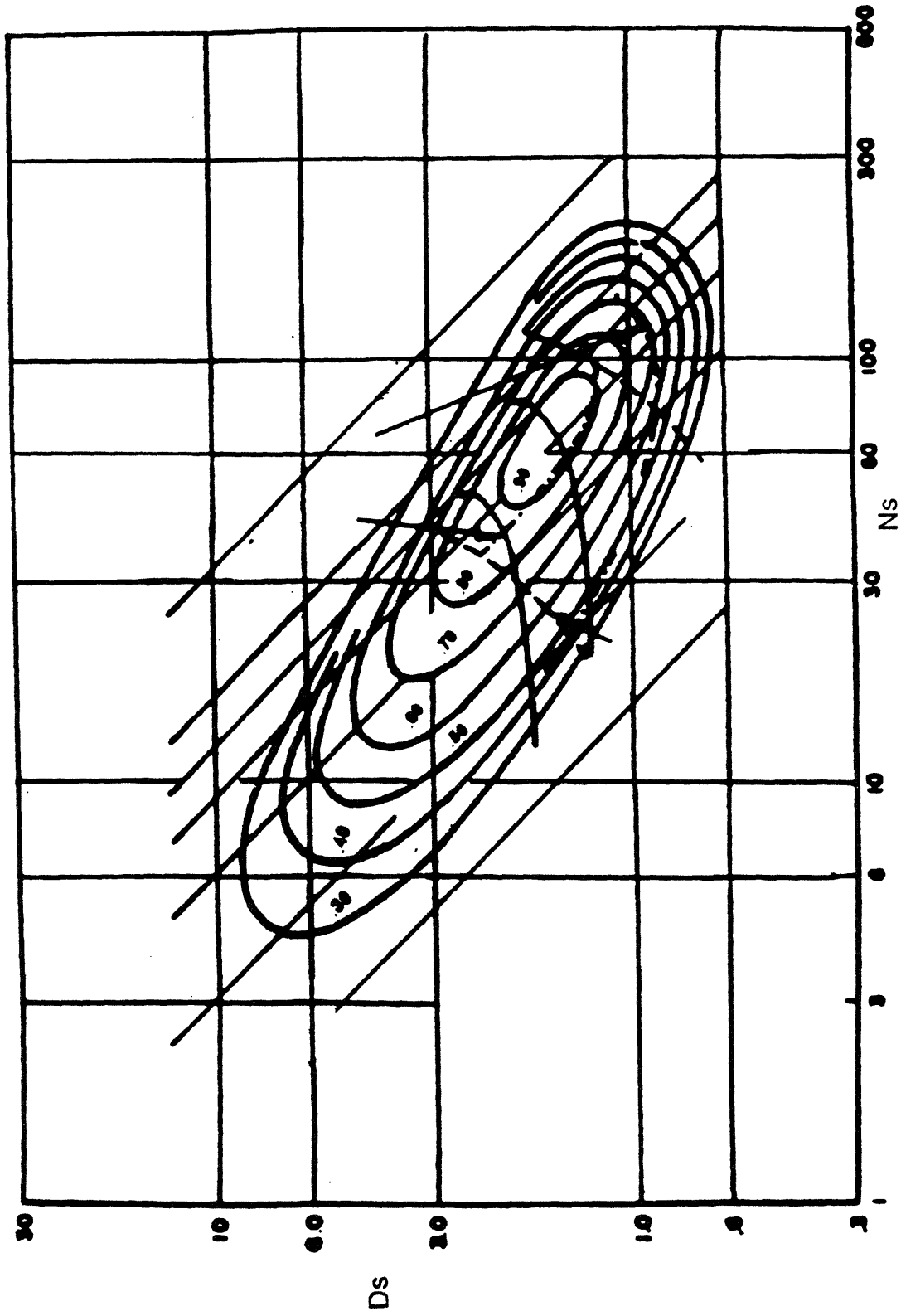

Fig. 2.9. Calculated Ns-Ds diagram for single stage radial turbines.

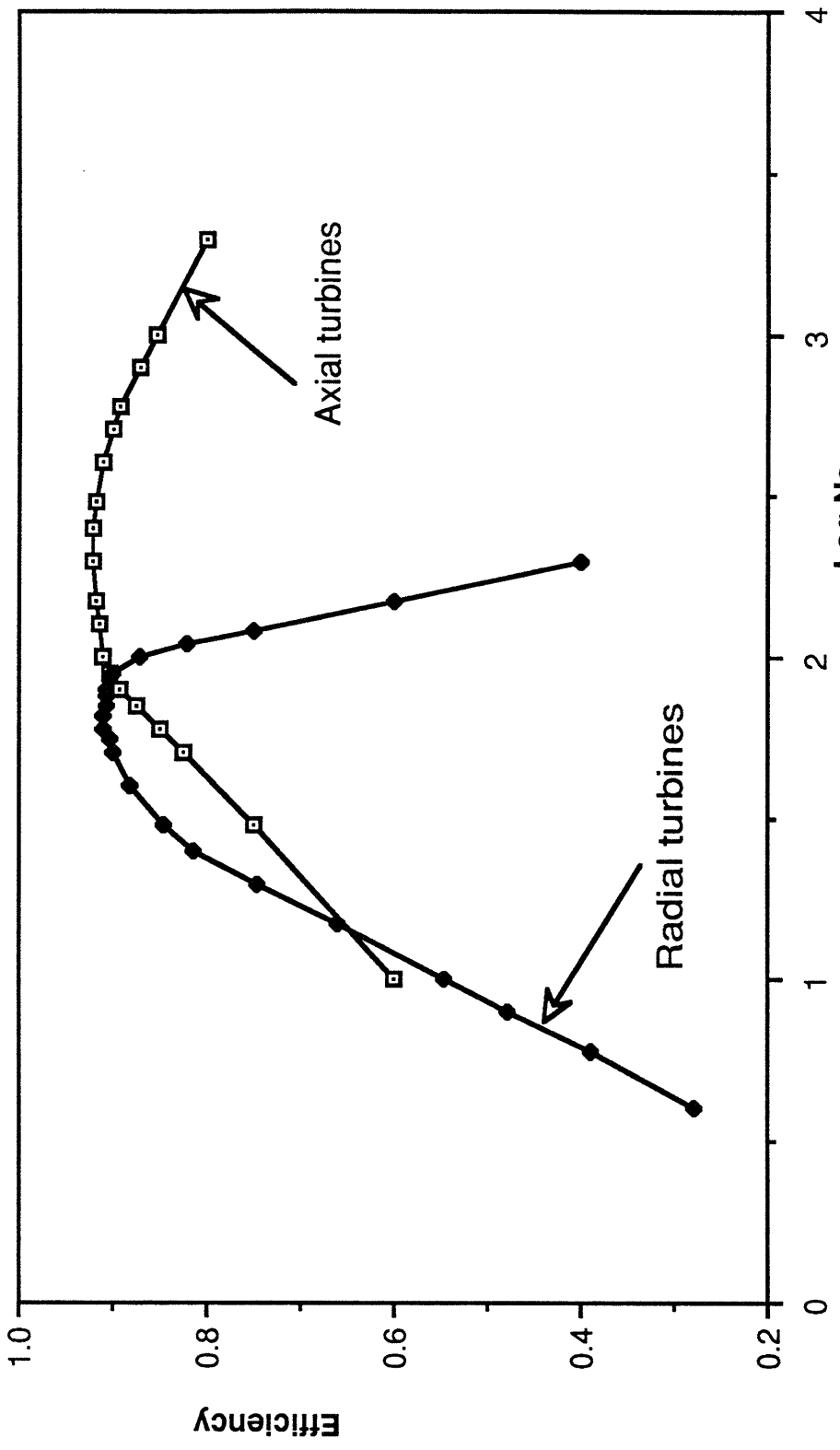

Fig. 2.10. Radial and axial turbines efficiency function of the specific speed.

CHAPTER 3

Discussion of Results

3.1. Turbine Weight:

In addition to the turbo-alternator-compressor efficiency, the weight is a very important parameter for space power generation systems. In reference [46] an empirical model was formulated. This model gives the specific weight, which is the weight of the engine per kilowatt. This empirical expression is given as follows:

$$F_t = 1.7844 \, (P_S)^{-0.292} \, (0.985)^{\Delta Y} \qquad (3.3)$$

Where:

F_t : is the specific weight in (kg/kw)

P_S: is the shaft power required (kw)

ΔY: is the years from 1958.

Since the maximum power in this thesis is 1Mw, one can calculate the specific weight and consequently the weight of the whole engine. The numerical application of (3.3) gives for (Ps = 1000 kw) a specific weight.

$$F_t = 0.1759 \text{ kg/kw}$$

and the total weight is:

$$We = 175.9 \text{ kg.}$$

If this weight is compared to that of the radiator and the nuclear reactor or the

solar collector and the other accessories, it will be found negligible. Therefore for space power generation systems, the weight of the turbo-alternator-compressor is not as important as its efficiency. Hence the curve of merit of these low power generation systems is the efficiency. For this reason it was the only parameter investigated in details in this subject.

3.2. Discussion and interpretation of the efficiency results:

Figure (2.10) was obtained by considering the maximum efficiency for the different specific speeds using the Ns-Ds diagrams. For specific speeds less than 50, the efficiency of both axial and radial turbines are low. For the radial turbines, as the specific speed gets lower, the specific diameter gets higher. We saw in equation (2.2) that the specific diameter was directly proportional to the rotor diameter. Increasing the disk diameter increases the disk friction losses, which cause the efficiency to drop to low values. For specific speeds between 50 and 90 the radial turbine efficiency is maximal, but it starts decreasing after Ns = 90, which makes Ns = 90 a higher limit for the radial turbines.

Concerning the axial turbines, the efficiency is low for specific speeds less than 90. At this range of specific speed the power output is less than 300 kw, which will be seen later, and the size of the turbine is very small which leads to a very small size of turbine blades. The construction of small turbine blades is very difficult; therefore the cost of the turbine gets very high

compared to that of a radial turbine. Another reason is that at small turbine sizes the clearance losses are very high, which lead to lower efficiencies and consequently the space power generation system gets heavier.
For specific speeds larger than 90, the radial turbine efficiency is much lower than that of the axial turbine. The axial turbine has maximum efficiencies for specific speeds greater than 90.

The specific speed was defined in the previous chapter as function of the volume flow, the rotational speed, and the head. In this chapter we give another definition to the specific speed. Balje, in reference [31], defined the specific speed as function of the rotational speed, the head, and the net power output as follows:

$$Ns = \frac{N}{H^{\frac{5}{4}}} \sqrt{\frac{P}{\rho \eta}} \qquad (3.1)$$

Where :

η : the turbine efficiency

ρ : the working fluid density

P : the net output power.

Sometimes the power is given in horsepower. Therefore we express the specific speed as function of the horsepower.
Since

1 HP = 745.7 watts

where:

HP: is the horsepower.

Then,

$$Ns = \frac{N}{H^{\frac{5}{4}}} \sqrt{\frac{745.7\ HP}{\rho \eta}} \qquad (3.2)$$

For given parameters of a turbine cycle, one can calculate the specific work (gH) of the given turbine. For a certain power level and rotational speed the specific speed can be calculated using equation (3.1) or equation (3.2). Returning to figure (2.10) obtained previously, the efficiencies of both radial and axial turbines can be read directly for the calculated Ns. Comparing the two efficiencies obtained , one can decide which turbine to choose.

Since the power output is directly related to the specific speed, it is a good idea to plot the specific speed verses the net power output.

Some data are taken from reference [19].

The turbine inlet temperature is $T_{tmax} = 1422\ ^{o}k$,

the compressor pressure ratio is $\pi_c = 2$,

The results are tabulated on table 3.1

The specific speed is plotted on figure (3.1.a) as function of the power output. To keep the specific speed greater than 60, we plotted it for different values of rotational speed. For power output between 1 kw and 20 kw, the rotational speed was taken 36000 rpm and the gas molecular weight was M=83.8. For power output between 20 kw and 50 kw, the rotational speed

was N=24000 rpm and the gas molecular weight M=83.8. For power output between 50 kw and 140 kw, the rotational speed was N=36000 rpm and M=40. For $P \geq 150$ kw, N=24000 rpm and M=40.

We saw on figure (2.10) that the radial turbines are more efficient than the axial turbines for specific speeds between 40 and 90.

Figure (3.1.a) shows that the specific speed reaches the value of 90 for power output P = 300 kw. Therefore one can conclude that the radial turbines are more efficient for power output between 1 kw and 300 kw. This is due to the fact that for turbine power less than 300 kw, the size of the axial turbine is small and the rotor diameter is very small, which leads to very small turbine blades. At this size the ratio of the clearance to the rotor diameter is relatively big, and consequently the clearance losses are pretty high. For power output greater than 300 kw the size of the axial turbine rotor becomes relatively big and the size of blades becomes big enough to be constructed, and the manufacturing cost becomes acceptable. As the output power increases the rotor diameter increases and the relative clearance gets smaller and consequently the clearance losses get smaller, which leads to a higher turbine efficiency.

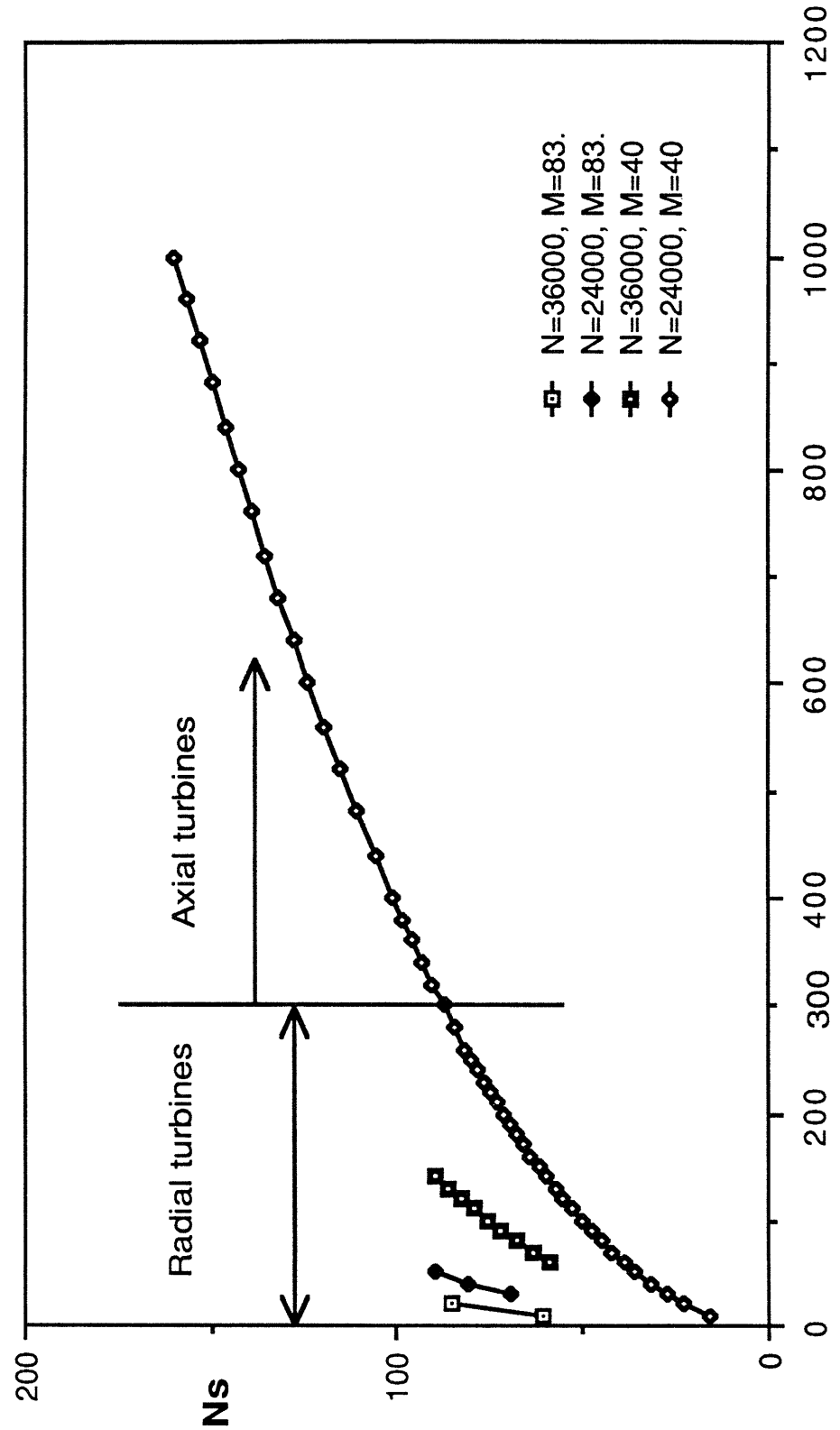

Fig. 3.1.a. Choice of the turbine type as function of the net output power

3.3. Application of the specific speed concept to Brayton and Rankine cycles:

3.3.1. Rankine cycle:

Rankine cycle systems use vapor as working fluid. On earth most Rankine-cycle power plants use water as working fluid and operate successfully. For space use, the most suitable fluids that can work at high temperatures are the alkali metals. Figure (3.1) shows the principle of work of the Rankine cycle.

The fluid is pumped back to the turbine by a pump which requires a small power to do such a work. Therefore the power that drives the pump is always considered negligible, and the power output is almost equal to the turbine power.

The specific speed is given by:

$$Ns = \frac{N}{H\overline{4}^{\frac{5}{4}}} \sqrt{\frac{745.7\ HP}{\rho\eta}} \qquad (3.3.1)$$

3.3.2. Brayton cycle:

Brayton cycle is a conventional closed gas turbine. In this type of cycles a compression is followed by heating at approximately constant pressure, first in the recuperator and finally in the heat source, where the gas is heated to the turbine inlet temperature. The gas is expanded through the turbine and is cooled along at an approximately constant pressure, first in

the recuperator and than in the heat waste radiator. The cycle is completed when the cooled gas enters the compressor.

The power developed by the turbine is divided into three parts. one part is the power lost, the second part is the power that drives the compressor, and the third part is the power output.
The compressor power is given by:

$$P_c = \dot{m}\, Cp\, \Delta T_c \qquad (3.3.2)$$

The turbine power is :

$$P_t = P_c + P_{out} \qquad (3.3.3)$$

Taking the power lost into consideration the turbine specific speed becomes:

$$Ns_t = \frac{N}{H_t^{5/4}} \sqrt{\frac{\dot{m}\, Cp\, \Delta T + P_{out}}{\eta\rho}} \qquad (3.3.4)$$

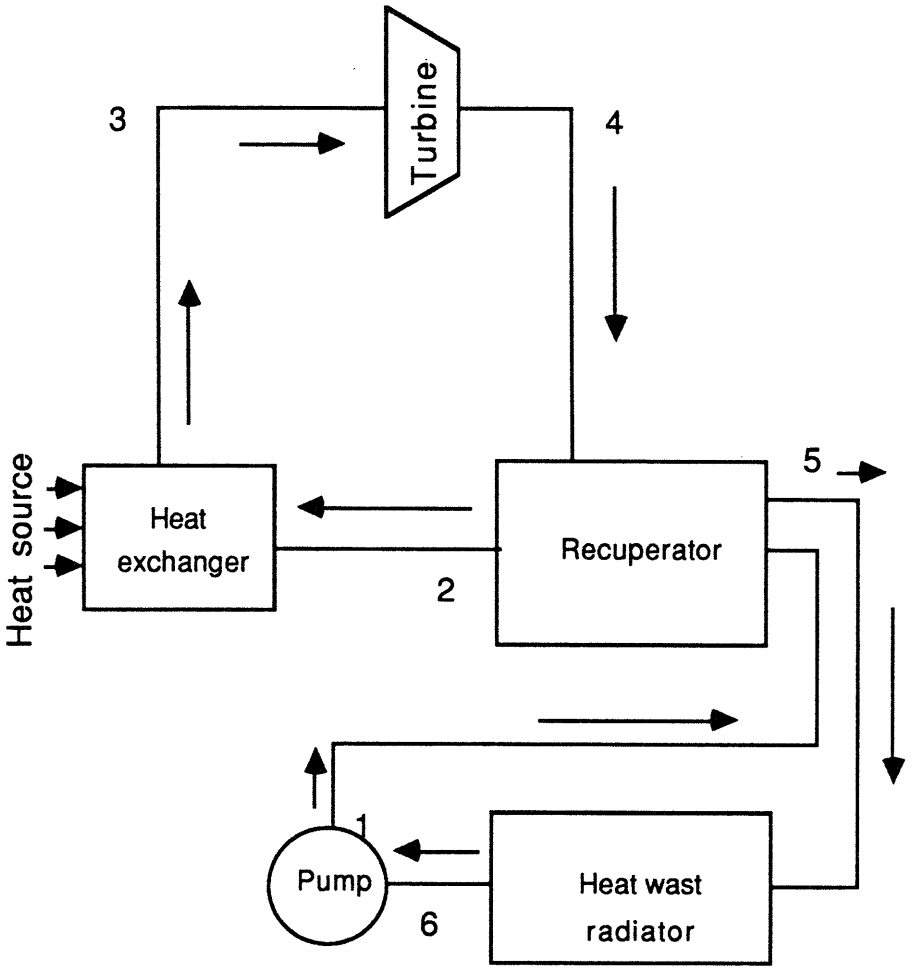

Fig. 3.1. Principle of work of Rankine cycle.

3.4. Optimization of the rotational speed N:

We defined previously that the specific turbine enthalpy was defined as:

$$H = Cp\ \Delta T \qquad (3.3)$$

We also defined Ns as function of the output power in equation (3.1).
The gas density is defined as function of the cycle parameters as:

$$\rho = p_3 / R\ T_3 \qquad (3.4)$$

Where:

R : is the gas constant, (J / kg ^{o}k)

Substituting (3.3) and (3.4) into (3.2) and for a given value of the turbine efficiency η, the specific speed becomes:

$$Ns = \frac{N}{(Cp\ \Delta T)^{5/4}} \sqrt{\frac{745.7\ HP\ .\ R\ .\ T_3}{\eta\ p_3}} \qquad (3.5)$$

For known power and turbine cycle parameters and for given rotational speed the specific speed can be calculated from the expression (3.5). From figure (2.10) the efficiency can be read for both types of turbines. With a comparison of the two efficiencies read, the type of turbine that has higher efficiency will be chosen for the system. After that we refer to figure (2.8) or (2.9) depending on the type of the turbine chosen. For either figures one can

read the specific diameter for Ns and η found.

Using equations (2.2) and (3.3) and with the fact that :

$$Q = \frac{\dot{m}}{\rho}$$

an expression of the rotor diameter can be given by:

$$D = \frac{Ds \sqrt{\dot{m} / \rho}}{(Cp\, \Delta T)^{1/4}} \qquad (3.6)$$

The tangential speed of the rotor is given by:

$$U = \pi D N / 60$$

This peripheral velocity cannot go beyond a certain limit for material resistance reason. As an example, for a certain material the peripheral speed is limited to:

$$U < 427 \text{ m / sec.}$$

Therefore,

$$D N < \frac{25620}{\pi} \qquad (3.7)$$

If equation (3.7) is not satisfied, either a smaller value of the rotational speed or a smaller specific diameter will be chosen, until (3.7) is satisfied. But for constant Ns the latter choice will be at the expense of the turbine efficiency.

3.5. Compressors Selection:

The efficiency of the compressor is a function of the specific speed and specific diameter. The procedure of obtaining compressors Ns-Ds diagrams is similar to that of the turbines. In these diagrams the lines of constant efficiencies are given as function of the specific diameter and the specific speed. Figure (3.2) is a combination of the diagrams of the radial, mixed flow and axial flow compressors. The dashed lines on the figure are the lines of constant efficiencies of the pumps.

On figure (3.3) it is clearly shown that the maximum radial compressor efficiency is obtained at specific speeds of 90 to 130, and specific diameters of 1.3 to 1.7.

The reason for limiting the range of specific speed for radial compressors to a lower limit of 90 is that the maximum efficiency decreases while decreasing the specific speed to values less than 90. The decrease of the efficiency is due to the fact that the hydraulic diameter of the impeller exit area is affected by the density change of the gas occurring in the impeller. The tendency is to decrease the impeller - discharge width with increasing design pressure ratio in order to obtain favorable velocity vectors. This usually causes the hydraulic diameter to decrease, and consequently the losses to increase with increasing pressure ratios. Another reason for limiting the specific speed is that the low specific speed compressors have relatively large disks which cause higher wheel-disk friction losses.

For specific speeds between 130 and 300 the mixed flow compressors have the highest efficiency. For specific speeds higher than 300 the most efficient types of compressors are the axial flow ones.

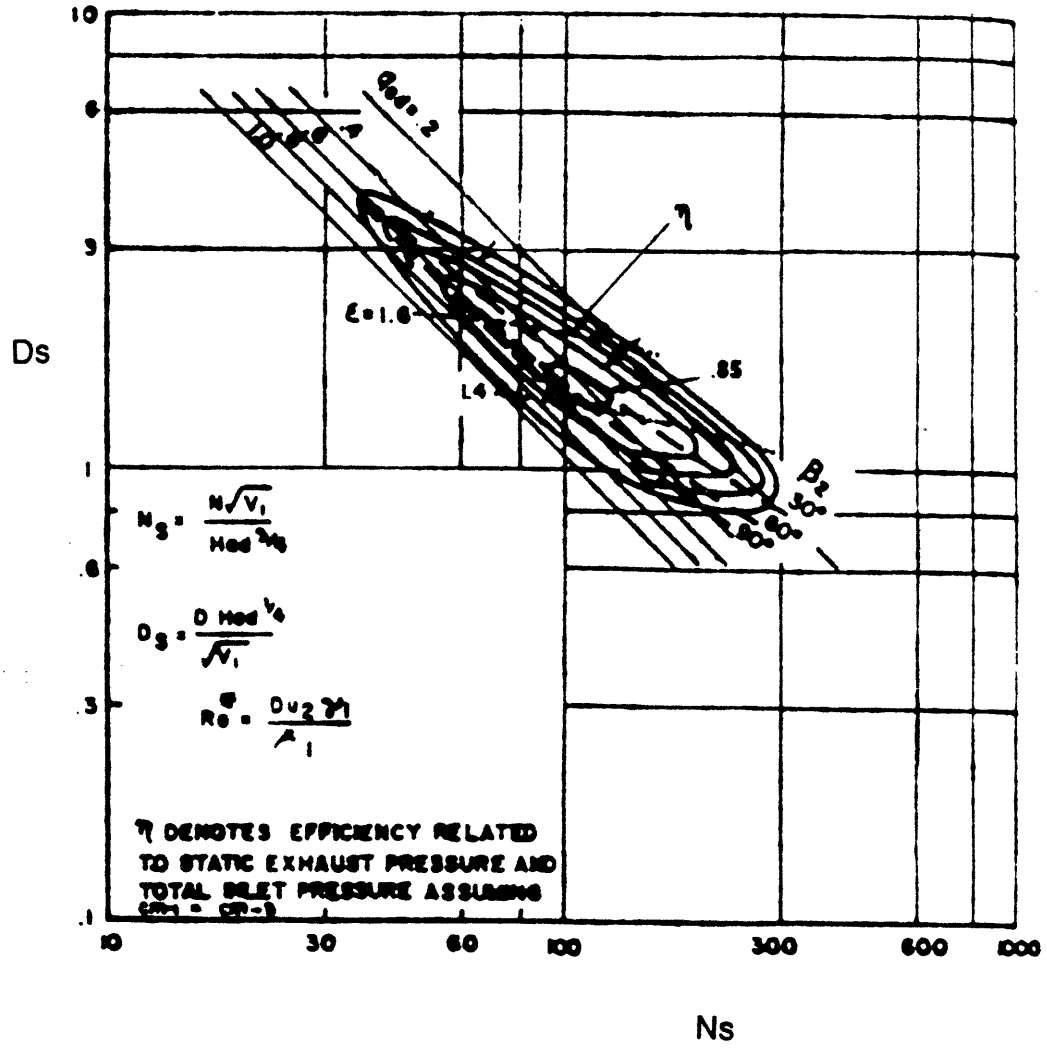

Fig.3.3. Ns Ds-diagram for radial compressors.

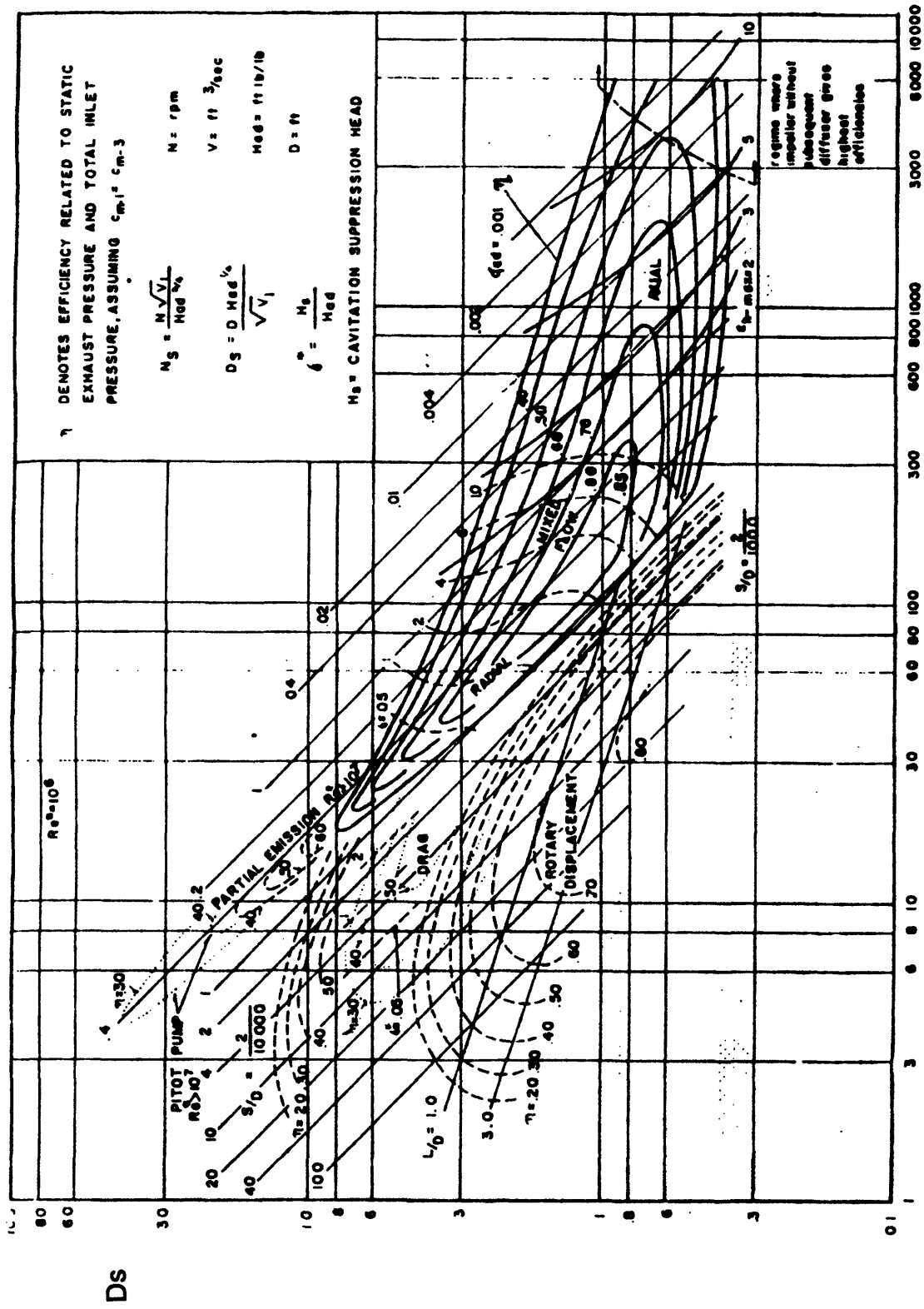

Fig. 3.2. Ns-Ds diagram for low-pressure-ratio compressors.

It was seen in chapter 2 that at power output of 160 kwe the radial and axial compressors were equal. Therefore for power output less or equal to 160 kwe, the radial compressors are the most efficient compressors. For power output larger than 160 kwe the mixed flow and axial compressors are more efficient than the radial ones.

3.6. Matching of the turbo-compressor unit :

The problem that the designers face is how to match the compressor with the turbine. Since the turbine and the compressor have the same weight flow for a closed cycle and their pressure ratios are interrelated, then there is a relationship between the compressor and the turbine specific speeds. For a single spool arrangement where the compressor and the turbine are directly interrelated, the ratio of their specific speeds is given by:

$$\frac{N_{s-c}}{N_{s-t}} = \sqrt{\frac{p_{3-t}}{p_{1-c}}} * \left(\frac{T_{1-t}}{T_{1-c}}\right)^{\frac{1}{4}} * \left(\frac{Y_t}{Y_c}\right)^{\frac{3}{4}} * \frac{1}{\sqrt{1 - Y_t \eta_t}} \qquad (3.8)$$

Where:

Y_t : is the turbine pressure ratio coefficient given by:

$$Y_t = 1 - \left(\frac{p_3}{p_1}\right)_t^{\frac{\gamma-1}{\gamma}} \qquad (3.9)$$

Y_c : is the compressor pressure ratio coefficient.

Equation (3.8) is plotted as function of the pressure ratio for ($T_{1t} / T_{1c} = 3$) and ($T_{1t} / T_{1c} = 4$). This variation is shown on figure (3.4).

Where (T1t / T1c) is the ratio of the turbine inlet temperature to the compressor inlet temperature.

For known pressure ratio and temperature ratio one can refer to figure (3.3) and determine the specific speed ratio. On figure (3.3) the lowest ratio of specific speeds is 1. Therefore one can conclude that the compressor specific speed is always greater than the turbine specific speed.

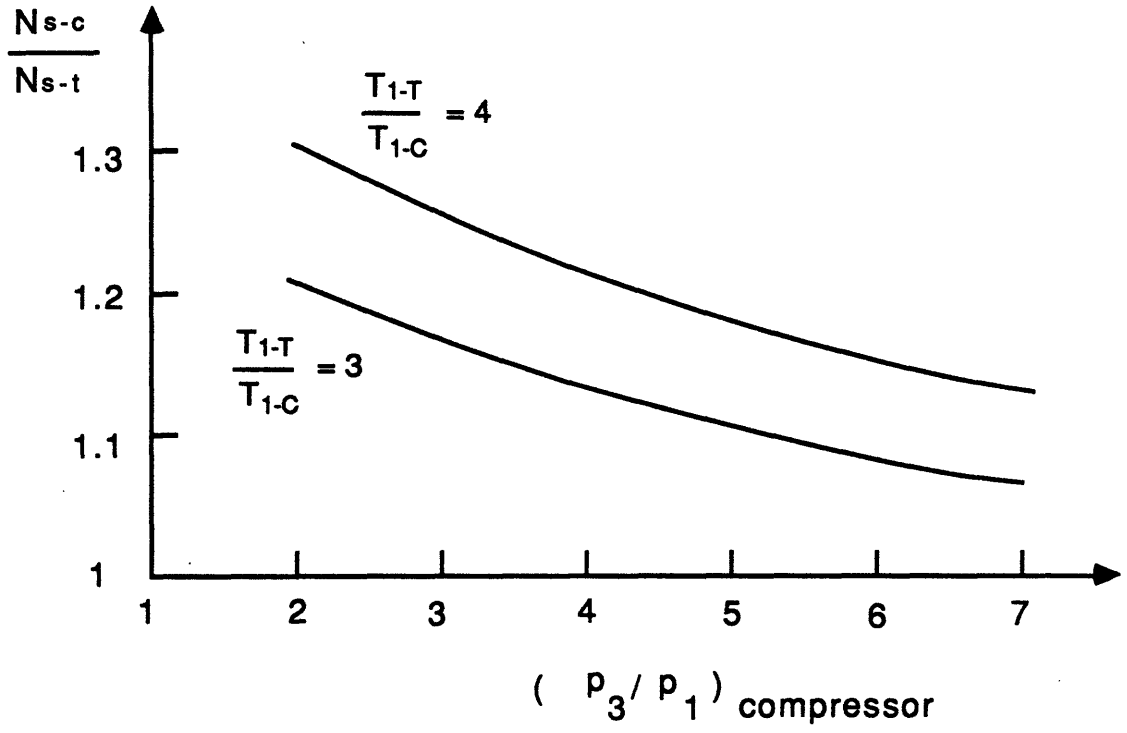

Fig. 3.4. Interrelation of specific speeds for single-spool gas turbines.

CHAPTER 4

Conclusion

The goal of this study was to make a comparison between the different types of turbines and compressors in terms of efficiency. The efficiency is proportional to the specific speed and specific diameter which are very important parameters in the design of turbomachinery.

A theoretical analysis for the different types of compressors and turbines was made first followed by some examples of turbo-compressor designs. The first example was the design of a 10 kwe turbo-compressor package designed by NASA, references [10, 11]. It was found that the radial compressor and the radial turbine were more efficient than the axial ones. After that a 15 kwe to 80kwe power generation system was investigated and the radial configuration for both the compressor and the turbine was chosen because of its high efficiency compared to that of the axial configuration. Finally a 160 kwe power generation system was investigated. The design was made by NASA reference [19]. It was found that the radial compressor and the axial compressor have the same efficiencies, and for cost reason, the radial configuration was chosen. The radial turbines were found more efficient than the axial turbines.

There are two important parameters for the design of turbomachinery for space power generation use. Those parameters are the weight and the efficiency of the turbo-alternator-compressor unit. An empirical model for the weight was formulated in reference [46]. The weight of a 1000 kwe turbo-compressor unit was 176 kg. If one compares this weight to that of the solar

collector and the heat exchangers, he would find it negligible. Therefore only the efficiency was taken as a curve of merit in this subject.

The maximum efficiency of the radial and axial turbines was plotted as a function of the specific speed using the NsDs-diagrams. Figure (2.10) shows that the radial turbines are more efficient than the axial turbines for specific speeds less than 90 and have maximum efficiency for specific speeds between 50 and 90. The axial turbines are more efficient than the radial turbines for specific speeds greater than 90.

The specific speed was also defined as a function of the net power output and was plotted for powers from 0 kw to 1 Mw. For power output of 300 kw the specific speed reaches the value of 90 which is the higher limit of specific speed for the radial turbines. For powers greater than 300 kw the specific speed is greater than 90. This implies that for power less than 300 kw the radial turbines are more efficient than the axial ones.

Finally NsDs-diagrams were used to determine the best types of compressors in terms of efficiency. For specific speeds between 90 and 130 the radial compressors are the most efficient ones. For specific speeds between 130 and 300 the mixed flow compressors are better than the others. For specific speeds greater than 300 the axial compressors are the most efficient types of compressors. The experimental data showed that the radial compressors remain more efficient than the other types as long as the net power output remains less than 160 kw. For net power output greater than this value the mixed flow and axial compressors are more efficient than the radial compressors.

As a final conclusion we set the following tables to summarize the results.

Power range	Type of compressor	Type of turbine
1 kw to 160 kw	Radial	Radial
160 kw to 300 kw	Mixed flow or axial	Radial
300kw to 1000kw	Axial	Axial

Specific speed range	Type of turbine
0 to 40	X
40 to 90	Radial turbine
> 90	Axial turbine

Specific speed range	Type of compressor
90 to 130	Radial
130 to 300	Mixed flow
> 300	Axial

Table 3.1. Summary of results

He-Xe Molecular Weight	83.8	60	40
Cp (J / Kg K)	248.2	346.67	520.0
h (kJ/kg)	63.705	88.975	133.463

Table 3.2. Working fluid characteristics.

REFERENCES

1. " Space Power Systems " , Advanced Technology Conference , NASA , SP - 131 , August 23-24 / 1966 .

2. "Power Generation from Nuclear Reactors in Aerospace Applications" NASA , TM 83342 , November 15-17 , 1982 .

3. " Turbine Design and Applications " , Volume I .
By Arthur J. Glassman
NASA SP-290.

4. "Turbine Design and Applications" , Volume II .
By Arthur J. Glassman
NASA SP-290.

5. " Status of the 2-to-15 kwe Brayton power system and potential gains from component improvements. "
By: John L. Klann , and William T. Wintucky.
(NASA) IECEC 1971

6. " Performance of a Brayton-cycle power conversion system using a Helium-Xenon gas mixture. "
By: Alfred S.Valerino and Lloyd W. Ream
(NASA) IECEC 1971.

7. "Experimental evaluation of the electrical subsystems of the 2 - to - 15 kwe Brayton power conversion system. "
By: R. R. Secunde, and J. E. Vracik, and A. C. Spagnuolo.
(NASA) IECEC 1971.

8. " Design point characteristics of a 15 - to - 80 kwe nuclear reactor Brayton-cycle power system. "
By: Paul T. Kerwin.
(NASA) ,IECEC, 1971

9. " Predicted performance of a 15 - 80 kwe reactor brayton power system over a range of operating conditions. " By: D .C. Guentert, and R.L. Johson (NASA) IECEC 1971.

10. " Design and Fabrication of the Brayton Cycle High Performance Turbine Research Package " .
NASA CR 72478 , Feb 14 , 1968 .

11. " Design and Fabrication of the Brayton Cycle High Performance Turbine Research Package " , NASA CR 72533 , Nov 29 , 1967 .

12. " 2 to 10 kw solar or radioisotope Brayton power system "
by John L. Klann.
IECEC , 1968 p. 407.

13. " Design and Fabrication of the BRU " ,
By: J.E. Davis .
NASA , CR 1870. March 1972

14. " Thermodynamics of Turbomachinery " , S.L. Dixon , 1978.

15. " Compressors Selection and Sizing " , Royce N. Brown , 1986.

16. " The Centrifugal Compressor Stage "
By: T.B. Ferguson , Gulf publishing company 1986.

17. " Estimating Centrifugal Compressor Performance " , Ronald P. Lapina , V 1 , Process Compressor Technology , 1982.

18. " Performance Prediction of Centrifugal Pumps and Compressors " , S. Gopalakrishnan , P. Cooper , C. Grennan and J. Switzer , ASME .

19. " Conceptual Design Study of a Nuclear Brayton Turboalternator - Compressor " , NASA , CR 113 925 .

20. " Final Report Design and Fabrication of the Brayton Cycle High Performance Turbine Research Package "
By: James H. Dunn , NASA , CR 72478 .

21. " Study of Brayton Cycle Power Generation System Using Snap-8 Nuclear Reactor as an Energy source " .
By: Donald C. Guentert and Roy L . Johnsen .
NASA , TN D 5751 , April 1970 .

22. " Centrifugal Compressors , Flow Phenomena and Performance " , Agard , TL 505 , N 867 , # 282 .

23. Fluid Mechanics for Engineers, by P. S. Barna. 1964.

24. " Gas Turbine Principle and Practice : The Radial Turbine " .
By: Cox . London George Newnes , 1955 .

25. " Principles of Turbomachinery. "
By: Shepherd ,
The Macmillan Company , New York 1956 , (Sixth Printing 1966) .

26. Turbomachines : A Guide to Design , Selection , and Theory. "
By: O.E.Balje'. John Willey & Sons , New York 1981 .

27. " Gas Turbine Theory. " By: Cohen. Great Britain , Hazell Watson and Viney Ltd , Second impression with Corrections 1974 .

28. " Principles of Turbomachinery. " By: R.K. Turton.
E & F.N. Spon Ltd , 1984 .

29. " Contribution to the Problem of Designing Radial Turbomachines " ,
O.E. Balje' , Transactions of the ASME , Vol 74 , 1953, pp 451 .

30. " Theoretical Assessment of the Performance Characteristics of
Inward Radial Flow Turbines " .
By: F.J. Wallace.
Proc. Instn. Mech. Engns. , London , Vol 172 , 1958 , pp 931 .

31. " A Study on Design Criteria and Matching of Turbomachines " ,
Part A - " Similarity Relations and Design Criteria of Turbines " ,
Part B - " Compressor and Pump Performance and Matching of
Turbo-components " .
By: O.E. Balje' , Journal of Engineering for Power , Transactions. of
the ASME , Vol 84 , 1962 , pp 83 - 114 .

32. " current Technology of Radial -Inflow Turbines for Compressible
Fluids " .
By: Homer J. Wood , Journal of Engineering for Power , Trans.
ASME , Vol 85 , series A , 1963 .

33. " Aircraft Engines and Gas Turbines " , Jack L. Kerrebrock , M.I.T.
Press .

34 " An Experimental Investigation of Centrifugal Compressor Surge and Stall Phenomena in Turbochargers " .
By: David A. Fink , S.M Thesis , May 1984 , M.I.T , Dept of Aeronautics & Astronautics.

35. " Experimental Performance Evaluation of a Radial - Inflow Turbine Over a Range of Specific Speeds. "
By: Milton G. Kofskey, and Charles A Wasserbauer.
NASA TN D - 3742, 1966.

36. " Analytical Determination of Radial Inflow Turbine Design Geometry for Maximum Efficiency. " By: Harold E. Rohlik.
NASA TN D - 4384, year 1968.

37. " Design of Turbines for High - Energy - Fuel - Low - Power - Output Applications."
By: Alan H. Stenning.
M.I.T. Dynamic Analysis and Control Lab. Report # 79 Sept. 1953.

38. " Technology for Brayton - Cycle Space Powerplants Using Solar and Nuclear Energy."
By: Robert E English.
NASA TN 2558 Feb. 1986.

39. " Aerodynamic Evaluation of Two-Stage Axial Flow Turbine DEsigned for Brayton Cycle Space Power System."
By: Milton G. Kofskey, and William J. Nusbaum.
NASA TN D - 4382 Feb. 1968.

40. " Pumping Characteristics of a Rotating Truncated Cone. "
By: Sol H. Gorland, and James C. Wood.
NASA TM X - 52953.

41. " Experimental Windage Losses for a Lundell Generator Operating in Air in the Turbulent Flow Regime."
By: Sol H. Gorland, and Erwin E. Kempke, Jr.
NASA TM X - 52905.

42. " Investigation of the Aerodynamic Performance of Small Axial Turbines ".
By: J.S.Ewen, F. W. Huber, and J. P. Mitchell.
ASME 73 - GT - 3.

43. " The Radial Turbine for Low Specific Speeds and Low Velocity Factors ".
By: E. M. Knoernschild.
Transactions of the ASME vol. 83 , 1961, series A, # 1, p.1.

44. " Preliminary Design of a High Temperature Solar Brayton Space Power System." By: George L. Wittinghill.
M.I.T. Report Space System Lab. #7 - 83. Feb. 1983.

45. " Brayton Cycle 3.2 - Inch Radial Compressor Performance Evaluation."
By: G. L. Perrone, and H. H. Milligan
NASA CR - 54968.

46. " Space Power Conversion Systems Using a Modified Ericsson Cycle With Turbomachinery."
By: Berner, Jeffry K. MS Thesis 1985. M.I.T.